

Constrained Geometry Organoactinides as Versatile Catalysts for the Intramolecular Hydroamination/Cyclization of Primary and Secondary Amines Having Diverse Tethered C–C Unsaturation

Bryan D. Stubbert and Tobin J. Marks*

Contribution from the Department of Chemistry, Northwestern University, Evanston, Illinois 60208-3113

Received September 14, 2006; E-mail: t-marks@northwestern.edu

Abstract: A series of “constrained geometry” organoactinide complexes, (CGC)An(NMe)₂ (CGC = Me₂-Si(η^5 -Me₄C₅)(^tBuN); An = Th, **1**; U, **2**), has been prepared via efficient in situ, two-step protodeamination routes in good yields and high purity. Both **1** and **2** are quantitatively converted to the neutrally charged, solvent-free dichlorides (**1**-Cl₂, **2**-Cl₂) and slightly more soluble diiodides (**1**-I₂, **2**-I₂) with excess Me₃Si-X (X = Cl, I) in non-coordinating solvents. The new complexes were characterized by NMR spectroscopy, elemental analysis, and (for **1** and **2**) single-crystal X-ray diffraction, revealing substantially increased metal coordinative unsaturation vs the corresponding Me₂SiCp''₂AnR₂ (Cp'' = η^5 -Me₄C₅; An = Th, R = CH₂-(SiMe₃), **3**; An = U, R = CH₂Ph, **4**) and Cp'₂AnR₂ (Cp' = η^5 -Me₅C₅; An = Th, R = CH₂(SiMe₃), **5**; An = U, R = CH₂(SiMe₃), **6**) complexes. Complexes **1**–**6** exhibit broad applicability for the intramolecular hydroamination of diverse C–C unsaturations, including terminal and internal aminoalkenes (primary and secondary amines), aminoalkynes (primary and secondary amines), aminoallenes, and aminodienes. Large turnover frequencies (*N*_t up to 3000 h⁻¹) and high regioselectivities ($\geq 95\%$) are observed throughout, along with moderate to high diastereoselectivities (up to 90% *trans* ring closures). With several noteworthy exceptions, reactivity trends track relative 5f ionic radii and ancillary ligand coordinative unsaturation. Reactivity patterns and activation parameters are consistent with a reaction pathway proceeding via turnover-limiting C=C/C \equiv C insertion into the An–N σ -bond.

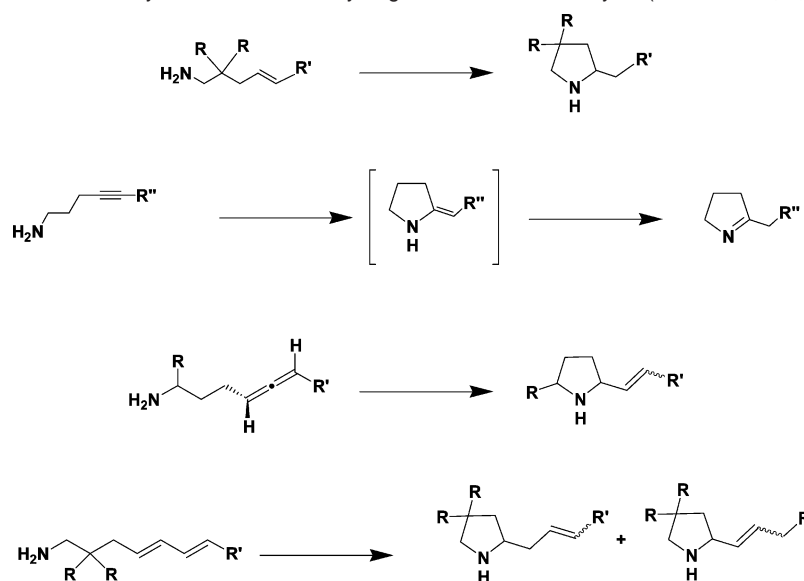
Introduction

The regioselective formation of C–N bonds is an important transformation in chemistry and biology, attracting considerable interest in both academic and industrial research.¹ Hydroamination (HA), defined as the formal addition of an N–H bond across a unit of C–C unsaturation,² is an atom-economical route to constructing both simple and complex organonitrogen skeletons and is capable of doing so efficiently and with high selectivity. Initially dominated by studies involving lan-

thanides,^{3,4} current *intramolecular* HA/cyclization research activity is wide-ranging² and spans the entire Periodic Table,^{5,6} from Ca⁷ to the coinage metals.⁸ While late transition metal catalysts generally enjoy greater functional group tolerance, they often require acidic conditions and *N*-protected amines and may

- (1) For general C–N bond-formation references, see: (a) Beller, M.; Seayad, J.; Tillack, A.; Jiao, H. *Angew. Chem., Int. Ed.* **2004**, *43*, 3368–3398. (b) Hartwig, J. F. *Science* **2002**, *297*, 1653–1654. (c) Beller, M.; Riermeier, T. H. In *Transition Metals for Organic Synthesis*, **1998**, *1*, 184–194. (d) Hegedus, L. S. *Angew. Chem., Int. Ed.* **1988**, *27*, 1113–1126. (2) For general hydroamination reviews, see: (a) Odom, A. L. *Dalton Trans.* **2005**, 225–233. (b) Hultzsich, K. C. *Adv. Synth. Catal.* **2005**, *347*, 367–391. (c) Hultzsich, K. C.; Gribkov, D. V.; Hampel, F. J. *Organomet. Chem.* **2005**, *690*, 4441–4452. (d) Hong, S.; Marks, T. J. *Acc. Chem. Res.* **2004**, *37*, 673–686. (e) Doye, S. *Synlett* **2004**, 1653–1672. (f) Beller, M.; Tillack, A.; Seayad, J. In *Transition Metals for Organic Synthesis*, 2nd ed.; Beller, M., Bohm, C., Eds.; Wiley-VCH: Weinheim, 2004; pp 91–94. (g) Roesky, P. W.; Mueller, T. E. *Angew. Chem., Int. Ed.* **2003**, *42*, 2708–2710. (h) Pohlki, F.; Doye, S. *Chem. Soc. Rev.* **2003**, *32*, 104–114. (i) Bytschkov, I.; Doye, S. *Eur. J. Org. Chem.* **2003**, *2003*, 935–946. (j) Seayad, J.; Tillack, A.; Hartung, C. G.; Beller, M. *Adv. Synth. Catal.* **2002**, *344*, 795–813. (k) Togni, A. In *Catalytic Heterofunctionalization*, 1st ed.; Togni, A., Gruetzmacher, H., Eds.; Wiley-VCH: New York, 2001; pp 91–141. (l) Nobis, M.; Driessen-Holscher, B. *Angew. Chem., Int. Ed.* **2001**, *40*, 3983–3985. (m) Eisen, M. S.; Straub, T.; Haskel, A. J. *Alloys Compd.* **1998**, *271*–273, 116–122. (n) Mueller, T. E.; Beller, M. *Chem. Rev.* **1998**, *98*, 675–703.

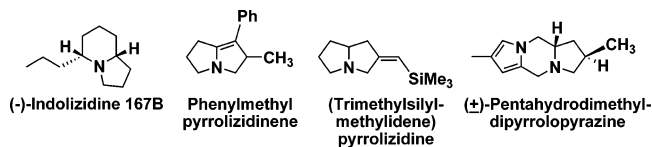
- (3) (a) Seyam, A. M.; Stubbert, B. D.; Jensen, T. R.; O'Donnell, J. J., III; Stern, C. L.; Marks, T. J. *Inorg. Chim. Acta* **2004**, *357*, 4029–4035. (b) Ryu, J.-S.; Marks, T. J.; McDonald, F. E. *J. Org. Chem.* **2004**, *69*, 1038–1052. (c) Hong, S.; Kawaoka, A. M.; Marks, T. J. *J. Am. Chem. Soc.* **2003**, *125*, 15878–15892. (d) Hong, S.; Tian, S.; Metz, M. V.; Marks, T. J. *J. Am. Chem. Soc.* **2003**, *125*, 14768–14783. (e) Ryu, J.-S.; Li, G. Y.; Marks, T. J. *J. Am. Chem. Soc.* **2003**, *125*, 12584–12605. (f) Hong, S.; Marks, T. J. *J. Am. Chem. Soc.* **2002**, *124*, 7886–7887. (g) Ryu, J.-S.; Marks, T. J.; McDonald, F. E. *Org. Lett.* **2001**, *3*, 3091–3094. (h) Arredondo, V. M.; Tian, S.; McDonald, F. E.; Marks, T. J. *J. Am. Chem. Soc.* **1999**, *121*, 3633–3639. (i) Arredondo, V. M.; McDonald, F. E.; Marks, T. J. *Organometallics* **1999**, *18*, 1949–1960. (j) Tian, S.; Arredondo, V. M.; Stern, C. L.; Marks, T. J. *Organometallics* **1999**, *18*, 2568–2570. (k) Arredondo, V. M.; McDonald, F. E.; Marks, T. J. *J. Am. Chem. Soc.* **1998**, *120*, 4871–4872. (l) Li, Y.; Marks, T. J. *J. Am. Chem. Soc.* **1998**, *120*, 1757–1771. (m) Roesky, P. W.; Stern, C. L.; Marks, T. J. *Organometallics* **1997**, *16*, 4705–4711. (n) Li, Y.; Marks, T. J. *J. Am. Chem. Soc.* **1996**, *118*, 9295–9306. (o) Li, Y.; Marks, T. J. *Organometallics* **1996**, *15*, 3770–3772. (p) Li, Y.; Marks, T. J. *J. Am. Chem. Soc.* **1996**, *118*, 707–708. (q) Giardello, M. A.; Conticello, V. P.; Brard, L.; Gagne, M. R.; Marks, T. J. *J. Am. Chem. Soc.* **1994**, *116*, 10241–10254. (r) Giardello, M. A.; Conticello, V. P.; Brard, L.; Sabat, M.; Rheingold, A. L.; Stern, C. L.; Marks, T. J. *J. Am. Chem. Soc.* **1994**, *116*, 10212–10240. (s) Li, Y.; Fu, P.-F.; Marks, T. J. *Organometallics* **1994**, *13*, 439–440. (t) Gagne, M. R.; Brard, L.; Conticello, V. P.; Giardello, M. A.; Stern, C. L.; Marks, T. J. *J. Am. Chem. Soc.* **1992**, *114*, 2003–2005. (u) Gagne, M. R.; Stern, C. L.; Marks, T. J. *J. Am. Chem. Soc.* **1992**, *114*, 275–294. (v) Gagne, M. R.; Marks, T. J. *J. Am. Chem. Soc.* **1989**, *111*, 4108–4109.

Scheme 1. Scope of Intramolecular HA/Cyclization Mediated by Organo-4f-Element Catalysts (See Refs 2d, 3, and 4)

be further plagued by low efficiency and short catalyst lifetimes.² Early transition metal catalysts typically exhibit enhanced activity; however, with one noteworthy exception,⁵ⁱ these electrophilic catalysts normally have limited functional group tolerance and sluggish reaction rates vs larger, more electrophilic organolanthanide catalysts.^{2–5}

Beginning with terminal aminoalkenes,^{3u,v} intramolecular organolanthanide-catalyzed HA/cyclization processes have been extensively investigated (Scheme 1),^{2d,3,4} typically displaying near-quantitative yields in addition to high regio- and diastereoselectivities (>95%) in addition to moderate/good enantioselectivities (up to 95%).^{2b–d,3b–d,q,r,4b,d,f,i–o,9} The highly exo-

thermic intramolecular HA/cyclization of simple aminoalkynes proceeds with surprising ease for both terminal and 1,2-disubstituted alkynes when catalyzed by organolanthanide complexes.^{3n,s} Furthermore, single amines tethered to C=C and C≡C linkages undergo cascade reactions involving sequential C–N/C–C bond fusions with high regioselectivity to afford indolizidine, pyrrole, pyrrolizidine, and pyrazine scaffolds, while



- (4) For additional examples of group 3- and lanthanide-catalyzed HA, see: (a) Bambirra, S.; Tsurugi, H.; van Leusen, D.; Hessen, B. *Dalton Trans.* **2006**, 1157–1161. (b) Gribkov, D. V.; Hultzsich, K. C.; Hampel, F. *J. Am. Chem. Soc.* **2006**, *128*, 3748–3759. (c) Panda, T. K.; Zulys, A.; Gamer, M. T.; Roesky, P. W. *Organometallics* **2005**, *24*, 2197–2202. (d) Collin, J.; Daran, J.-C.; Jacquet, O.; Schulz, E.; Trifonov, A. *Chem. Eur. J.* **2005**, *11*, 3455–3462. (e) Kim, J. Y.; Livinghouse, T. *Org. Lett.* **2005**, *7*, 4391–4393. (f) Kim, J. Y.; Livinghouse, T. *Org. Lett.* **2005**, *7*, 1737–1739. (g) Molander, G. A.; Hasegawa, H. *Heterocycles* **2004**, *64*, 467–474. (h) Lauterwasser, F.; Hayes, P. G.; Brase, S.; Piers, W. E.; Schafer, L. L. *Organometallics* **2004**, *23*, 2234–2237. (i) Hultzsich, K. C.; Hampel, F.; Wagner, T. *Organometallics* **2004**, *23*, 2601–2612. (j) O'Shaughnessy, P. N.; Gillespie, K. M.; Knight, P. D.; Munslow, I. J.; Scott, P. *Dalton Trans.* **2004**, 2251–2256. (k) O'Shaughnessy, P. N.; Scott, P. *Tetrahedron: Asymmetry* **2003**, *14*, 1979–1983. (l) O'Shaughnessy, P. N.; Knight, P. D.; Morton, C.; Gillespie, K. M.; Scott, P. *Chem. Commun.* **2003**, 1770–1771. (m) Kim, Y. K.; Livinghouse, T.; Horino, Y. *J. Am. Chem. Soc.* **2003**, *125*, 9560–9561. (n) Molander, G. A.; Pack, S. K. *Tetrahedron* **2003**, *59*, 10581–10591. (o) Molander, G. A.; Pack, S. K. *J. Org. Chem.* **2003**, *68*, 9214–9220. (p) Kim, Y. K.; Livinghouse, T. *Angew. Chem., Int. Ed.* **2002**, *41*, 3645–3647. (q) Bürgstein, M. R.; Berberich, H.; Roesky, P. W. *Chem. Eur. J.* **2001**, *7*, 3078–3085. (r) Kim, Y. K.; Livinghouse, T.; Bercaw, J. E. *Tetrahedron Lett.* **2001**, *42*, 2933–2935. (s) Molander, G. A.; Dowdy, E. D. *J. Org. Chem.* **1999**, *64*, 6515–6517. (t) Molander, G. A.; Dowdy, E. D. *J. Org. Chem.* **1998**, *63*, 8983–8988.
- (5) For group 4 catalysts see: (a) Thomson, R. K.; Bexrud, J. A.; Schafer, L. L. *Organometallics* **2006**, *25*, 4069–4071. (b) Lee, A. V.; Schafer, L. L. *Organometallics* **2006**, *25*, 5249–5254. (c) Esteruelas, M. A.; Lopez, A. M.; Mateo, A. C.; Onate, E. *Organometallics* **2006**, *25*, 1448–1460. (d) Bexrud, J. A.; Beard, J. D.; Leitch, D. C.; Schafer, L. L. *Org. Lett.* **2005**, *7*, 1959–1962. (e) Esteruelas, M. A.; Lopez, A. M.; Mateo, A. C.; Onate, E. *Organometallics* **2005**, *24*, 5084–5094. (f) Kim, H.; Lee, P. H.; Livinghouse, T. *Chem. Commun.* **2005**, 5205–5207. (g) Hoover, J. M.; Petersen, J. R.; Pikul, J. H.; Johnson, A. R. *Organometallics* **2004**, *23*, 4614–4620. (h) Gribkov, D. V.; Hultzsich, K. C. *Angew. Chem., Int. Ed.* **2004**, *43*, 5542–5546. (i) Knight, P. D.; Munslow, I.; O'Shaughnessy, P. N.; Scott, P. *Chem. Commun.* **2004**, 894–895. (j) Li, C.; Thompson, R. K.; Gillon, B.; Patrick, B. O.; Schafer, L. L. *Chem. Commun.* **2003**, 2462–2463. (k) Ackermann, L.; Bergman, R. G. *Org. Lett.* **2002**, *4*, 1475–1478. (l) Ackermann, L.; Bergman, R. G.; Loy, R. N. *J. Am. Chem. Soc.* **2003**, *125*, 11956–11963.

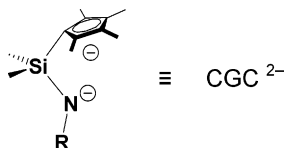
selectively retaining unsaturations amenable to subsequent functionalization.^{3j,l,p,n,4o,p} Initial difficulties in directly adding N–H bonds across 1,2-disubstituted C=C linkages^{3i,u,4s,t} were overcome via implementation of more open, thermally robust organolanthanide structures at high temperatures.^{3b,h,4o} En route to such advances, heterocyclic skeletons of greater structural complexity were accessed from allenic^{3h,i,k} and dienic^{3c,d,f} substrates. In all cases, the tunable ionic radii of the lanthanide series (Table 1)¹⁰ proved vital to understanding those kinetic

- (6) See for example: (a) Krogstad, D. A.; Cho, J.; DeBoer, A. J.; Klitzke, J. A.; Sanow, W. R.; Williams, H. A.; Halfen, J. A. *Inorg. Chim. Acta* **2006**, *359*, 136–148. (b) Zhang, J.; Yang, C.-G.; He, C. *J. Am. Chem. Soc.* **2006**, *128*, 1798–1799. (c) Kadzimirsz, D.; Hildebrandt, D.; Merz, K.; Dyker, G. *Chem. Commun.* **2006**, 661–662. (d) Bajracharya, G. B.; Huo, Z.; Yamamoto, Y. *J. Org. Chem.* **2005**, *70*, 4883–4886. (e) Field, L. D.; Messerle, B. A.; Vuong, K. Q.; Turner, P. *Organometallics* **2005**, *24*, 4241–4250. (f) Bender, C. F.; Widenhoefer, R. A. *J. Am. Chem. Soc.* **2005**, *127*, 1070–1071. (g) Zulys, A.; Dochnahl, M.; Hollmann, D.; Löhnwitz, K.; Herrmann, J.-S.; Roesky, P. W.; Blechert, S. *Angew. Chem. Int. Ed.* **2005**, *44*, 7794–7798. (h) Lutete, L. M.; Kadota, I.; Yamamoto, Y. *J. Am. Chem. Soc.* **2004**, *126*, 1622–1623. (i) Schlummer, B.; Hartwig, J. F. *Org. Lett.* **2002**, *4*, 1471–1474.
- (7) Crimmin, M. R.; Casely, I. J.; Hill, M. S. *J. Am. Chem. Soc.* **2005**, *127*, 2042–2043.
- (8) (a) Kadzimirsz, D.; Hildebrandt, D.; Merz, K.; Dyker, G. *Chem. Commun.* **2006**, 661–662. (b) Zhang, J.; Yang, C.-G.; He, C. *J. Am. Chem. Soc.* **2006**, *128*, 1798–1799. (c) Muller, T. E.; Grosche, M.; Herdtweck, E.; Pleier, A.-K.; Walter, E.; Yan, Y.-K. *Organometallics* **2000**, *19*, 170–183.
- (9) For reviews of enantioselective catalysis with lanthanides, see: (a) Aspinall, H. C. *Chem. Rev.* **2002**, *102*, 1807–1850. (b) Inanaga, J.; Furuno, H.; Hayano, T. *Chem. Rev.* **2002**, *102*, 2211–2225. (c) Molander, G. A. *Pure Appl. Chem.* **2000**, *72*, 1757–1761.
- (10) Shannon, R. D. *Acta Crystallogr.* **1976**, *A32*, 751–67.

Table 1. Comparison of Ionic Radii for Relevant Lanthanide and Actinide Ions (See Ref 10)

ion	coordination no.	ionic radius (Å)
Th ⁴⁺	9	1.09
U ⁴⁺	9	1.05
La ³⁺	8	1.16
Sm ³⁺	8	1.079
Y ³⁺	8	1.019
Lu ³⁺	8	0.977

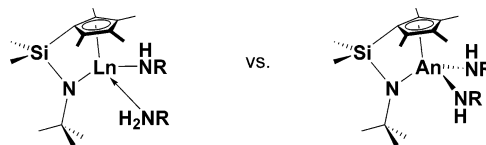
and mechanistic factors governing HA ring closure. Furthermore, the possibility of broadening the scope of this powerful C–N bond-forming methodology by tuning ancillary ligand architecture motivated the exploratory synthesis of additional catalyst classes. With open coordination spheres having documented applications throughout the Periodic Table,¹¹ the “constrained geometry” ligand (“CGC”) was applied to organolanthanides. The resulting catalysts are particularly efficacious for activating sterically encumbered and otherwise less-reactive amine substrates, especially when combined with larger radius lanthanides.^{3a–j}



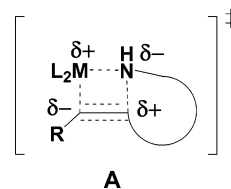
Actinide (An) and lanthanide (Ln) chemistries differ primarily in the degree of covalency and extent of f-orbital participation in bonding and reactivity.^{12,13} Unlike the poorly shielded and primarily nonbonding Ln 4f orbitals, limited involvement of An 6d and 5f orbitals has been invoked to explain observed molecular geometries and stabilities, as well as unique chemical reactivity patterns,¹⁴ and has been ascribed to the increased importance of relativistic effects^{12a,h–1} and improved shielding of the 5f orbitals. Although 6d and 5f orbital participation is still *relatively* modest, the degree of bond covalency in actinides is significantly enhanced over that in lanthanides,¹² presenting unique possibilities for new and interesting reactivity modalities.

- (11) For reviews of constrained geometry catalysts, see: (a) Gromada, J.; Carpentier, J.-F.; Mortreux, A. *Coord. Chem. Rev.* **2004**, *248*, 397–410. (b) Okuda, J. *Dalton Trans.* **2003**, 2367–2378. (c) Arndt, S.; Okuda, J. *Chem. Rev.* **2002**, *102*, 1953–1976. (d) Britovsek, G. J. P.; Gibson, V. C.; Wass, D. F. *Angew. Chem., Int. Ed.* **1999**, *38*, 428–447.
- (12) For reviews of 4f- and 5f-element chemistry, see: (a) Burns, C. J.; Neu, M. P.; Boukhalfa, H.; Gutowski, K. E.; Bridges, N. J.; Rogers, R. D. In *Comprehensive Coordination Chemistry II*, 1st ed.; McCleverty, J. A., Meyer, T. J., Eds.; Elsevier Pergamon: Amsterdam, 2004; Vol. 3, pp 189–345. (b) Edelmann, F. T.; Freckmann, D. M. M.; Schumann, H. *Chem. Rev.* **2002**, *102*, 1851–1896. (c) Molander, G. A.; Dowdy, E. D. *Top. Organomet. Chem.* **1999**, *2*, 119–154. (d) Edelmann, F. T. *Angew. Chem., Int. Ed.* **1995**, *34*, 2466–88. (e) Edelmann, F. T. In *Comprehensive Organometallic Chemistry II*; Abel, E. W., Stone, F. G. A., Wilkinson, G., Eds.; Pergamon: New York, 1995; Vol. 4, pp 11–213. (f) Schaverien, C. J. *Adv. Organomet. Chem.* **1994**, *36*, 283–362. (g) Molander, G. A. *Chem. Rev.* **1992**, *92*, 29–68. (h) *The Chemistry of the Actinide Elements*; Katz, J. J., Seaborg, G. T., Morss, L. R., Eds.; Chapman and Hall: New York, 1986. (i) *Fundamental and Technological Aspects of Organo-f-Element Chemistry*; Marks, T. J., Fraga, I. L., Eds.; Reidel: Dordrecht, 1985. (j) Marks, T. J.; Ernst, R. D. In *Comprehensive Organometallic Chemistry*; Abel, E. W., Stone, F. G. A., Wilkinson, G., Eds.; Pergamon: New York, 1982; Vol. 3, pp 173–270. (k) Marks, T. J. *Chemistry and Spectroscopy of f Element Organometallics, Part II. The Actinides. Progress in Inorganic Chemistry* **1979**, *25*, 224. (l) Marks, T. J. *Chemistry and Spectroscopy of f Element Organometallics, Part I. The Lanthanides. Progress in Inorganic Chemistry* **1978**, *24*, 51.
- (13) (a) Cotton, F. A.; Wilkinson, G.; Murillo, C. A.; Bochmann, M. *Advanced Inorganic Chemistry*, 6th ed.; John Wiley & Sons, Inc.: New York, 1999. (b) Kettle, S. F. A. *Physical Inorganic Chemistry: A Coordination Chemistry Approach*; Oxford University Press: New York, 1998. (c) Huheey, J. E.; Keiter, E. A.; Keiter, R. L. *Inorganic Chemistry: Principles of Structure and Reactivity*, 4th ed.; HarperCollins College Publishers: New York, 1993.

In light of the broad scope of substrates amenable to intramolecular HA/cyclization catalyzed by organolanthanides^{2d,3,4} along with the intriguing similarities and differences between 4f- and 5f-element organometallic chemistries,¹² the investigation of organoactinide HA/cyclization catalysts having increased coordinative unsaturation, along with an additional covalently bonded ligand (vs Ln), offers an ideal opportunity to examine the roles of bond covalency, ionic radius, metal oxidation state, and ancillary ligation, as well as the mechanistic significance of these factors.



We previously communicated the synthesis and characterization of several members of a new class of CGC organoactinide complexes, along with initial investigations of their catalytic competence for intramolecular HA/cyclization.¹⁵ From these preliminary results, we envisioned a mechanistic pathway as depicted in Scheme 2, with an insertive transition state such as **A**. In this contribution, we report improved syntheses of



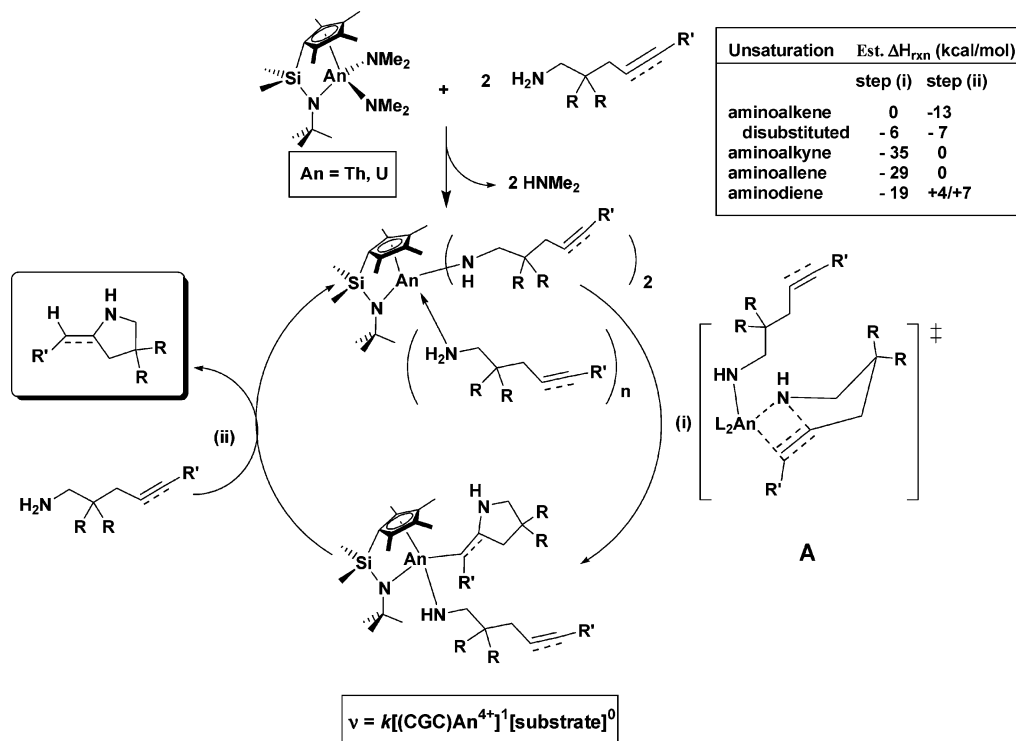
(CGC)An(complexes and a detailed investigation of their catalytic intramolecular HA/cyclization activity with respect to a broad series of representative substrates. We compare/contrast these results relative to electrophilic organolanthanide and group 4 metal catalysts. The scope of organoactinide-catalyzed HA/cyclization established includes 1,2-disubstituted alkenes, alkenes, and diene C–C unsaturations tethered to primary (1°) amines. Furthermore, we show that secondary (2°) aminoalkenes and aminoalkynes are rapidly converted to tertiary (3°) pyrrolidine and enamine heterocycles, *requiring* the agency of an M–N σ -bonded intermediate in the insertive transition state (**A**, Scheme 2). In a companion contribution, we present a detailed mechanistic investigation of (CGC)An(-mediated HA).¹⁶

Experimental Section

General Considerations. All manipulations of air-sensitive materials were carried out with rigorous exclusion of oxygen and moisture in flame- or oven-dried Schlenk-type glassware on a dual-manifold Schlenk line, interfaced to a high-vacuum manifold (10^{–6} Torr), or in

- (14) See, for example: (a) Barnea, E.; Eisen, M. S. *Coord. Chem. Rev.* **2006**, *250*, 855–899. (b) Burns, C. J. *Science* **2005**, *309*, 1823–1824. (c) Evans, W. J.; Kozimor, S. A.; Ziller, J. W. *Science* **2005**, *309*, 1835–1838. (d) Castro-Rodriguez, I.; Meyer, K. *J. Am. Chem. Soc.* **2005**, *127*, 11242–11243. (e) Evans, W. J.; Kozimor, S. A.; Ziller, J. W.; Kaltsoyannis, N. *J. Am. Chem. Soc.* **2004**, *126*, 14533–14547. (f) Castro-Rodriguez, I.; Nakai, H.; Zakharov, L. N.; Rheingold, A. L.; Meyer, K. *Science* **2004**, *305*, 1757–1760. (g) Castro-Rodriguez, I.; Nakai, H.; Gantzel, P.; Zakharov, L. N.; Rheingold, A. L.; Meyer, K. *J. Am. Chem. Soc.* **2003**, *125*, 15734–15735. (h) Diaconescu, P. L.; Arnold, P. L.; Baker, T. A.; Mindiola, D. J.; Cummins, C. C. *J. Am. Chem. Soc.* **2000**, *122*, 6108–6109.
- (15) Stubbert, B. D.; Stern, C. L.; Marks, T. J. *Organometallics* **2003**, *22*, 4836–4838.
- (16) Stubbert, B. D.; Marks, T. J. *J. Am. Chem. Soc.* **2007**, *129*, in press.

Scheme 2. Proposed Mechanism for the Intramolecular HA/Cyclization of C–C Unsaturations Tethered to 1° and 2° Amines, Including Alkene, Alkyne, Allene, and Diene Substrates under Mild Conditions in C₆D₆ or C₇D₈^a



^a This mechanistic scenario is consistent with the observed rate law, $v \sim [(CGC)An]^1[substrate]^0$, and is similar to the σ -bond insertive pathway proceeding through an $L_2Ln-N(H)R$ intermediate proposed for organolanthanide-catalyzed HA/cyclization processes (see refs 2–4).

a nitrogen-filled Vacuum Atmospheres glovebox with a high-capacity recirculator (<2 ppm of O₂). Argon (Matheson, prepurified) was purified by passage through a MnO oxygen-removal column and a Davison 4A molecular sieve column. All solvents were dried and degassed over Na/K alloy and transferred in vacuo immediately prior to use. All substrates for catalytic experiments were dried at least three times as solutions in benzene-*d*₆ or toluene-*d*₈ over freshly activated Davison 4A molecular sieves and were degassed by repeated freeze–pump–thaw cycles. Aminoalkynes were predried by stirring over BaO overnight as C₆D₆ solutions before rigorous drying over freshly activated molecular sieves. Substrates were then stored under Ar in vacuum-tight storage flasks. Full experimental details for improved syntheses of substrates **21**, **25**, and **41**, as well as **1-X**₂ and **2-X**₂, are provided in the Supporting Information.

Physical and Analytical Measurements. NMR spectra were recorded on a UNITYInova-500 (FT, 500 MHz, ¹H; 125 MHz, ¹³C) instrument. Chemical shifts (δ) for ¹H and ¹³C spectra are referenced to internal solvent resonances and reported relative to SiMe₄. NMR experiments on air-sensitive samples were conducted in Teflon valve-sealed tubes (J. Young). EI-HRMS data were obtained using a Thermo Finnigan MAT-XL900 spectrometer at 70 eV. Elemental analyses on air-sensitive samples were performed at the Micro-Mass Facility at the University of California, Berkeley; air-stable samples were analyzed at Midwest Microlabs (Indianapolis, IN).

(CGC)Th(NMe₂)₂ (1). A small flip-frit apparatus with a magnetic stir bar was charged in the glovebox with ThCl₄ (5.00 g, 13.4 mmol) and LiNMe₂ (2.65 g, 52.0 mmol, 3.9 equiv). After the system was evacuated under high vacuum, pentane (10 mL) and THF (60 mL) were condensed onto the solids at –196 °C. The stirring mixture was allowed to slowly warm to 20 °C under Ar and allowed to react for an additional 24 h before all volatiles were removed in vacuo. Pentane (30 mL) was condensed onto the resulting oily residue at –78 °C and then allowed to warm to 20 °C under Ar. After stirring overnight, the pale-yellow pentane solution was filtered and concentrated in vacuo to afford an

off-white solid that was further dried under high vacuum to afford 1.895 g of a roughly 1:1 mixture of Th(NMe₂)₄ and Li[Th(NMe₂)₅](THF)_{*n*}, as determined by ¹H NMR spectroscopy (ca. 4.64 mmol of “Th(NMe₂)₄”, 35% yield).¹⁷

A 100 mL round-bottom flask in the glovebox containing the isolated mixture (homoleptic amide + ate complex), a magnetic stir bar, and a high-vacuum adapter was charged with pentane (15 mL) and H₂CGC (1.18 g, 4.67 mmol) at 20 °C. The flask was moved to the high-vacuum manifold, where volatile byproduct HNMe₂ was periodically removed via Ar flush and/or partial evacuation over 3 d. Complete evacuation of volatiles, followed by condensation of fresh solvent (either pentane or toluene) into the reaction flask at –196 °C, was carried out once every 12 h. Reaction progress can be monitored by ¹H NMR spectroscopy. The product was next isolated by extraction with pentane (2 × 25 mL) and filtration. The solution was concentrated to a volume of ca. 10 mL, and **1** was isolated by slow cooling to –78 °C. Collection of the colorless powder on a glass frit afforded 1.94 g of **1** (74% yield based on “Th(NMe₂)₄”). ¹H NMR (C₆D₆, 500 MHz, 25 °C): δ 2.81 (s, 12 H, N(CH₃)₂), 2.20 (s, 6 H, C₅(CH₃)₄), 2.02 (s, 6 H, C₅(CH₃)₄), 1.30 (s, 9 H, NC(CH₃)₃), 0.67 (s, 6 H, Si(CH₃)₂). Anal. Calcd: C, 40.06; H, 6.90; N, 7.38. Found: C, 39.84; H, 6.90; N, 7.35.

(CGC)U(NMe₂)₂ (2). The one-pot preparative route to (CGC)An(NR₂)₂ complexes is detailed here for complex **2**. A 250 mL sidearm flask with a magnetic stir bar was charged in the glovebox with UCl₄ (3.00 g, 7.90 mmol) and LiNMe₂ (1.57 g, 30.8 mmol, 3.9 equiv). The flask was evacuated under high vacuum before pentane (20 mL) and THF (80 mL) were condensed onto the solids at –78 °C. The dark red mixture was protected from light and allowed to warm slowly with stirring to 20 °C under Ar.¹⁷ After 20 h, the volatiles were removed in vacuo and replaced with pentane (80 mL) at –78 °C. The mixture was warmed to 20 °C, and a solution of H₂CGC (2.35 g, 9.34 mmol, 1.18 equiv) in pentane (5 mL) was added by syringe through the sidearm

(17) Jamerson, J. D. Ph.D. Thesis, University of Alberta, 1974.

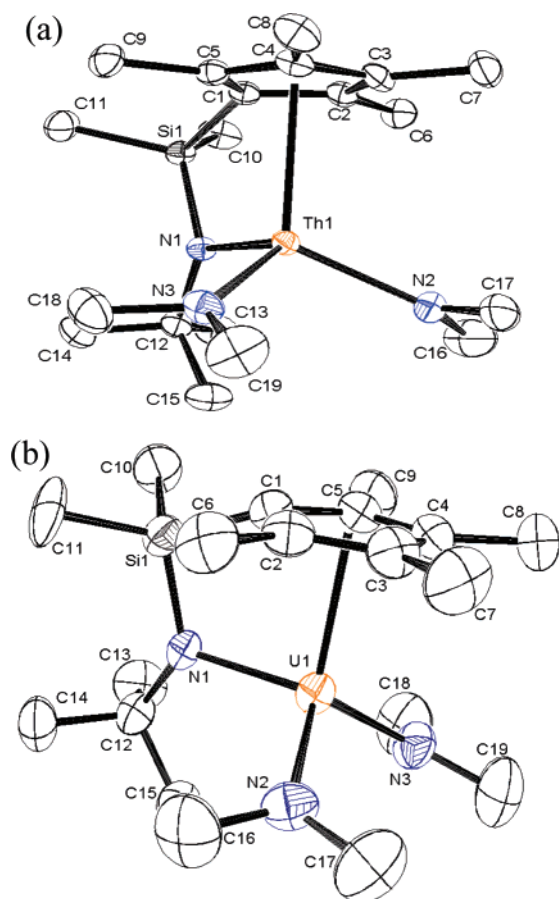


Figure 1. Solid-state structures of (CGC)An(NMe₂)₂ complexes and selected bond distances (Å) and angles (°). (a) Complex **1**, distances: Cp^{*}-(centroid)-Th, 2.498; Th-N1, 2.315(4); Th-N2, 2.266(5); Th-N3, 2.273(5). Angles: N2-Th-N3, 107.6(2); N1-Th-N2, 114.0(2); N1-Th-N3, 112.8(2). (b) Complex **2**, distances: Cp^{*}(centroid)-U, 2.425; U-N1, 2.278(4); U-N2, 2.207(4); U-N3, 2.212(4). Angles: N2-U-N3, 109.6(2); N1-U-N2, 111.0(2); N1-U-N3, 114.2(2). Ellipsoids are drawn at 50% probability (see ref 15).

under a rapid Ar purge. Byproduct HNMe₂ was periodically removed via Ar flow and/or partial evacuation over 2 d. Complete evacuation of volatiles, followed by condensation of fresh pentane into the flask at -196 °C, was carried out once every 6–12 h. Reaction progress can be monitored by ¹H NMR spectroscopy. Product **2** was isolated and purified by filtration, followed by concentration to a volume of <10 mL and slow cooling to -78 °C. Decantation of the mother liquor afforded 3.20 g of brown microcrystalline **2** in 71% yield (from UCl₄). ¹H NMR (C₆D₆, 500 MHz, 25 °C): δ 22.24 (s, 12 H, N(CH₃)₂), 15.28 (s, 6 H, C₅(CH₃)₄), 1.31 (s, 6 H, C₅(CH₃)₄), -18.93 (s, 9 H, NC(CH₃)₃), -22.08 (s, 6 H, Si(CH₃)₂). Anal. Calcd: C, 39.64; H, 6.83; N, 7.30. Found: C, 38.37; H, 6.75; N, 7.27.

Kinetic Studies of Hydroamination Reactions. In a typical experiment, the precatalyst (ca. 1–6 mg, 2–11 μmol) and the internal standard Si(*p*-tolyl)₄ (ca. 2–5 mg, 5–12 μmol) were dissolved in C₆D₆ (0.80 mL) and added to a Teflon-valved NMR tube in the glovebox. A preliminary ¹H NMR spectrum was recorded to verify the relative concentrations of precatalyst and standard. The NMR tube was then attached to a high-vacuum manifold via a glass adapter with a secondary Teflon valve and was placed in a -78 °C bath before being evacuated to ca. 5 × 10⁻⁶ Torr and resealed. The upper portion of the valve was then backfilled with Ar, and a 1 M solution of substrate in C₆D₆ (0.20 mL) was added to the adapter under a flush of Ar. The primary valve was next opened and the substrate solution pulled into the NMR tube, freezing the substrate solution just above the precatalyst solution. After

the tube was evacuated and backfilled with Ar three times, the valve was closed. The sample remained frozen in the -78 °C bath until it was thawed and placed directly into the Varian UNITYInova 500 MHz NMR spectrometer, pre-equilibrated at 25.0 °C (±0.2 °C), calibrated with a neat ethylene glycol standard. Data were obtained with only a single transient to avoid signal saturation, and substrate and/or product concentrations were determined relative to the intensity of an internal standard resonance, typically downfield of C₆D₃H in the aromatic region of Si(*p*-tolyl)₄ (7.74 ppm), over three or more half-lives. All data were fit by least-squares analysis according to eq 1, where C₀ is the initial concentration of substrate and *t* is time. The turnover frequency (*N_t*) was calculated according to eq 2, where *E* is the normalized substrate:catalyst ratio determined from the relative intensities of non-overlapping resonances in each ¹H NMR spectrum, typically with ±5% precision.

$$C = mt + C_0 \quad (1)$$

$$N_t = \left(\frac{m}{-C_0} \right) E \quad (2)$$

Results

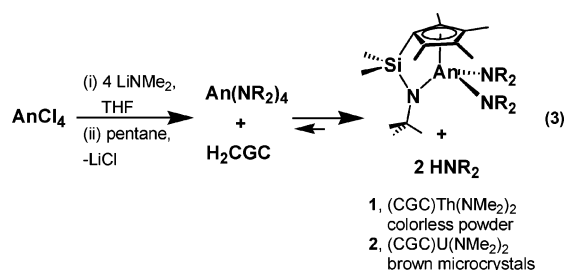
In this section we begin with an account of (CGC)AnX₂ synthesis, molecular structures, and reaction chemistry. We then discuss the intramolecular HA/cyclization of representative terminal and internal aminoalkene, aminoalkyne, aminoallene, and aminodiene substrates mediated by constrained geometry organoactinide complexes, as well as by other organoactinides of progressively less coordinative unsaturation. Catalytic reactions with terminal and 1,2-disubstituted 1° and 2° aminoalkenes are discussed in detail. Intramolecular terminal and 1,2-disubstituted alkyne HA/cyclization with both 1° and 2° amines is then described, followed by extension of the reaction scope to an illustrative selection of aminoallenes and aminodienes. The effects of both metal ionic radius and ancillary ligation are analyzed in each instance, along with relevant kinetic and activation parameters for ring closure involving each C–C unsaturation.

(CGC)AnX₂ Synthesis and Characterization. Constrained geometry organoactinide complexes **1** and **2** are prepared in good yields (ca. 70%) and high purity from AnCl₄ reagents via an improved, general procedure using the corresponding in situ generated homoleptic tetrakis(dialkylamido)actinide complexes, followed by protodeaminative substitution with the diprotic H₂CGC proligand (eq 3). NMR-scale syntheses proceed in quantitative yield and in >95% purity (¹H NMR spectroscopy), indicating that the yield-limiting step in (CGC)An(NR₂)₂ preparation is precipitation and crystallization from alkane or aromatic solvents. Yields are optimized by incorporating a slight stoichiometric excess of H₂CGC, counteracting the formation of ate complex contaminants (i.e., Li[An(NMe₂)₅(THF)_{*n*}], An = Th, U) and driving the product-forming equilibrium to the right (eq 3). Pentane-insoluble impurities (primarily residual LiCl) are removed by filtration prior to -78 °C recrystallization to afford analytically pure (CGC)An(NMe₂)₂ complexes **1** and **2**. The absence of coordinated Lewis bases in the final products allows direct application as precatalysts without further purification.^{3a,18} The solid-state structures of **1** and **2**, determined by single-crystal X-ray diffraction (Figure 1), are

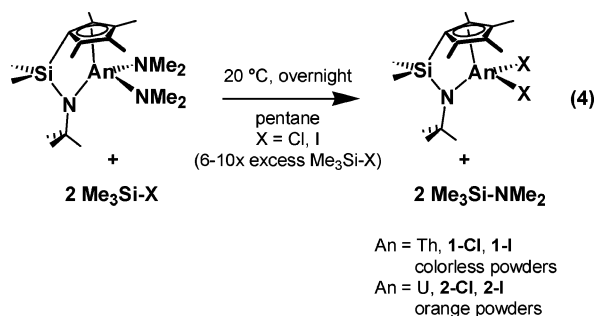
(18) Gillespie, R. D.; Burwell, R. L., Jr.; Marks, T. J. *Langmuir* **1990**, *6*, 1465–1477.

(19) EIMS (M⁺) data show fragments of *m/z* > MW_{monomer}, suggesting that (CGC)AnX₂ are dimeric (or trimeric) species. See Supporting Information for experimental details.

discussed below in the context of their substantially more open ligand frameworks and the impact on catalytic properties (vide infra).



Neutrally charged Lewis base-free halide complexes **1-Cl**₂, **2-Cl**₂, **1-I**₂, and **2-I**₂ are cleanly prepared by reaction of **1** or **2** with a 6–10-fold excess of Me₃Si–X (X = Cl, I; eq 4) in non-coordinating solvents. The dihalides are isolated cleanly and quantitatively from pentane as fine powders. Although the solubility of diiodides **1-I**₂ and **2-I**₂ is greater than that of dichlorides **1-Cl**₂ and **2-Cl**₂ in Et₂O and THF, insolubility in suitable non-coordinating solvents precludes cryoscopic molecular weight determination.¹⁹



Hydroamination/Cyclization. Substrate and Catalyst Trends. In this section, we present the results of catalytic intramolecular HA studies for a range of C–C unsaturations, revealing an impressive scope rivaled only by organolanthanide catalysts. Substrates surveyed with precatalysts **1–6** include primary (**7–18**) and secondary (**19–24**) terminal aminoalkenes, primary internal (**27–32**) aminoalkenes, primary (**33–42**) and secondary (**25, 26**) aminoalkynes, primary aminoallenes (**43–48**), and primary aminodienes (**49–54**).

(a) **Aminoalkenes.** Intramolecular HA/cyclization of terminal as well as 1,2-disubstituted (internal) amino-olefins is effectively mediated by (CGC)An⟨ complexes. Results for simple 1° amine substrates are presented first, followed by 2° amines and internal olefins. The scope of precatalyst **1**- and **2**-mediated terminal aminoalkene HA is summarized in Table 2. Thus, unsubstituted substrate **7** is converted to exocyclic product **8** by either **1** or **2** at roughly comparable *N_t* values, although rather sluggishly at 60 °C (Table 2, entries 1 and 2). Introduction of geminal dimethyl substituents in **9**→**10** cyclization (Table 2, entries 3 and 4) effects a reactivity increase of ca. 10× for **1** (*N_t* = 15 h⁻¹, An = Th) vs **2** (*N_t* = 2.5 h⁻¹, An = U) at 25 °C. A similar, though more pronounced effect is observed for **11**→**12**, where geminal disubstitution effects are enhanced by phenyl substitution (Table 2, entries 5 and 6). Here, precatalyst **1** effects HA/cyclization with remarkable efficiency at 25 °C – *N_t* = 1460 h⁻¹ as compared to the impressive *N_t* = 430 h⁻¹ for **2**. Again,

Table 2. Aminoalkene HA/Cyclization Processes Catalyzed by (CGC)An⟨ Complexes **1** and **2** in C₆D₆ Showing the Effects of Ionic Radius on *N_t*

Entry	Substrate	Product ^a	Precatalyst	<i>N_t</i> , h ⁻¹ (°C) ^b
1.			(CGC)Th(NMe ₂) ₂	0.3 (60)
2.	7	8	(CGC)U(NMe ₂) ₂	0.3 (60)
3.			(CGC)Th(NMe ₂) ₂	15 (25)
4.	9	10	(CGC)U(NMe ₂) ₂	2.5 (25)
5.			(CGC)Th(NMe ₂) ₂	1460 (25)
6.	11	12	(CGC)U(NMe ₂) ₂	430 (25)
7.			(CGC)Th(NMe ₂) ₂	0.2 (60)
8.	13	14	(CGC)U(NMe ₂) ₂	0.2 (60)
9.			(CGC)Th(NMe ₂) ₂	12 (60)
10.	15	16	(CGC)U(NMe ₂) ₂	15 (25)
11.			(CGC)Th(NMe ₂) ₂	4.3 (25)
12.	17	18	(CGC)U(NMe ₂) ₂	4.8 (25)

^a Yields ≥95% by ¹H NMR spectroscopy. ^b Determined by ¹H NMR spectroscopy.

the Th-based complex mediates the transformation with markedly greater efficiency, presumably owing to the larger ionic radius (Table 1, vide infra).

Larger piperidine rings are also accessible using the present organoactinide precatalysts. Again, the marked influence of geminal dialkyl substitution is evident, effecting a ca. 10× increase in *N_t* on going from substrate **13** to **15** to **17** when mediated by **1** for R = H < Me < Ph (entries 7, 9, and 11). The formation of five-membered pyrrolidine vs six-membered piperidine rings is significantly more efficient in most cases for either Th or U, with the notable exception of substrate **15**, where HA/cyclization proceeds *faster* for **2** than for **1** (at 25 °C for An = U vs 60 °C for An = Th). Compared with substrate **9** (*N_t* = 2.5 h⁻¹ at 25 °C; Table 2, entry 4), this pronounced difference in reactivity is intriguing and may reflect Th vs U electronic properties or unique steric factors introduced by the CGC ancillary ligand (vide infra). This effect also obtains for R = Ph substitution in substrate **17**, where *N_t* = 4.8 h⁻¹ at 25 °C (Table 2, entry 12). The results for **13** and **17** cyclization to piperidines **14** and **18**, respectively (Table 2, entries 7, 8, 11, and 12), parallel those for pyrrolidine formation and suggest that similar Th and U losses in cyclization efficiency are operative upon increasing the product ring size from five to six members.

The consequences of the steric openness of (CGC)An⟨ relative to more encumbered actinocene complexes are particularly evident in Table 3. Here, transformations **9**→**10** (entries 7–10) and **11**→**12** (entries 1–6) are compared for precatalysts **1–6**. Note that Cp′₂An⟨ complexes **5** and **6** display markedly diminished efficiencies and require heating at 60 °C for useful

Table 3. Aminoalkene HA/Cyclization of Substrates **9** and **11** Catalyzed by Organoactinide Complexes **1–6**. Comparison of N_t as a Function of Metal Ionic Radius and Ancillary Ligand Environment in C_6D_6

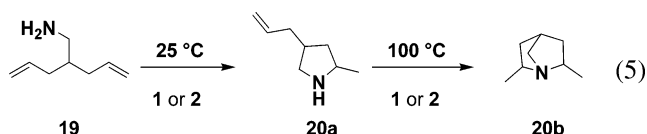
Entry	Substrate	Product ^a	Precatalyst	N_t , h^{-1} ($^{\circ}C$) ^b
1.			(CGC)Th(NMe ₂) ₂	1460 (25)
2.			(CGC)U(NMe ₂) ₂	430 (25)
3.			(Me ₂ SiCp'') ₂ ThR ₂	120 (25)
4.	11	12	(Me ₂ SiCp'') ₂ UR ₂	29 (25)
5.			Cp'') ₂ ThR ₂	2.8 (60)
6.			Cp'') ₂ UR ₂	1.0 (60)
7.			(CGC)Th(NMe ₂) ₂	15 (25)
8.			(CGC)U(NMe ₂) ₂	2.5 (25)
9.			Cp'') ₂ ThR ₂	0.4 (60)
10.	9	10	Cp'') ₂ UR ₂	0.2 (60)

^a Yields $\geq 95\%$ by ¹H NMR spectroscopy. ^b Determined by ¹H NMR spectroscopy.

HA/cyclization of the two most reactive aminoalkene substrates, **9** ($N_t = 0.4 h^{-1}$, An = Th; $N_t = 0.2 h^{-1}$, An = U; entries 9 and 10) and **11** ($N_t = 2.8 h^{-1}$, An = Th; $N_t = 1.0 h^{-1}$, An = U; entries 5 and 6). This reactivity–coordinative unsaturation trend is evident in comparing these results with those for precatalysts **3** and **4**, having intermediate Me₂SiCp'')₂An< ancillary ligation. With the extremely reactive substrate **11** ($N_t = 120 h^{-1}$, An = Th; $N_t = 29 h^{-1}$, An = U at 25 $^{\circ}C$; entries 3 and 4), the greater than 10 \times reactivity difference between complexes **1** vs **3** and **2** vs **4** is illustrative of the importance of the ancillary ligation and substrate accessibility to the catalytic center.

A representative plot of normalized [substrate]:[An] ratio vs time (Figure 2a) was determined from the ¹H NMR spectral intensities of precatalyst + Si(*p*-tolyl)₄ internal standard solutions. The slope of the plot is constant in all cases, indicating zero-order dependence on [substrate]. Near complete conversion (low [substrate]), some departure from linearity is observed. However, plots of multiple catalytic runs with a single loading of precatalyst in a single NMR tube (Figure 2b) indicate that this deviation is caused not by catalyst deactivation, but rather by competitive inhibitory binding of product, interfering with turnover-limiting C=C insertion into the An–N bond.^{2d,3u}

The cyclization of more complex 2 $^{\circ}$ amine substrates to form products containing 3 $^{\circ}$ amine skeletons was also explored for (CGC)An< complexes **1** and **2** (Table 4). Aminodiene **19** undergoes initial HA and cyclization to form the intermediate 2 $^{\circ}$ amine **20a** with an efficiency analogous to that for the structurally similar substrate **9** ($N_t = 12 h^{-1}$, An = Th and $N_t = 1.5 h^{-1}$, An = U; Table 4 entries 1 and 2). Interestingly, subsequent reaction at 100 $^{\circ}C$ cleanly converts **20a** to bicyclic **20b** in quantitative yield (eq 5). The 2 $^{\circ}$ amine analogue of



substrate **11**, *N*-methyl substrate **21**, displays the greatest turnover frequency of all aminoalkene transformations in Table

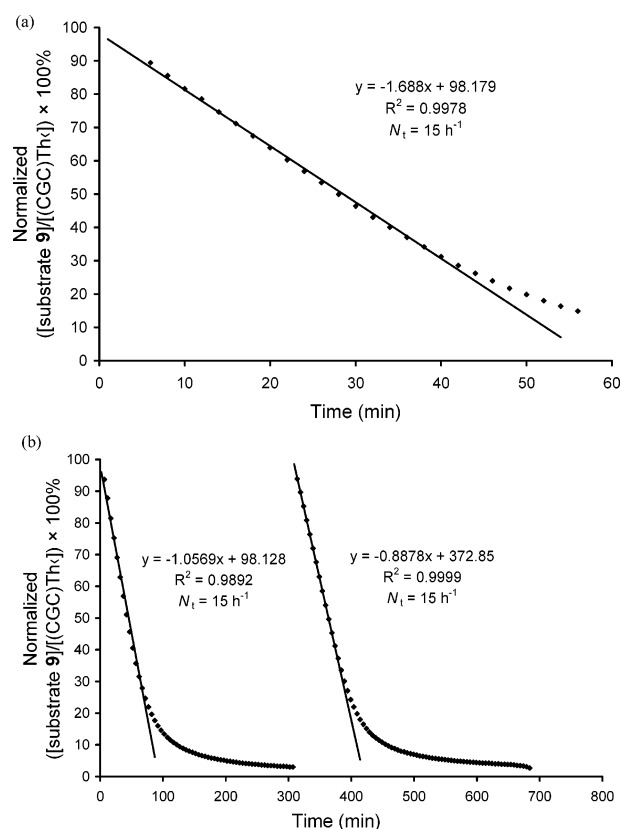


Figure 2. Kinetic plots for representative HA/cyclization of aminoalkenes. (a) Plot of the normalized ([aminoalkene **9**]/[(CGC)Th(\cdot)] ratio $\times 100\%$ ([CGC)Th(\cdot)] from precatalyst **1** relative to Si(*p*-tolyl)₄ internal standard) at 25 $^{\circ}C$ in C_6D_6 . The line depicts the least-squares fit, with N_t determined from the slope of the line according to eqs 1 and 2. (b) Plot of ([aminoalkene **9**]/[(CGC)Th(\cdot)] $\times 100\%$ (normalized to Si(*p*-tolyl)₄ internal standard) over two consecutive catalytic runs under identical conditions. Following completion of the first HA/cyclization reaction, all volatiles were removed in vacuo (including product **10**; 10^{-6} Torr) and replaced with fresh C_6D_6 solvent and fresh substrate **9** (see Experimental Section for complete details).

4 and proceeds smoothly at 60 $^{\circ}C$ ($N_t = 0.6 h^{-1}$, An = Th; $N_t = 0.8 h^{-1}$, An = U; entries 5 and 6). Sterically more encumbered **23** bears an *N*-benzyl substituent and requires 100 $^{\circ}C$ reaction temperatures to achieve significant rates ($N_t = 0.1 h^{-1}$; Table 4, entries 7 and 8). The steric and electronic obstacles presented by **23** are reflected in the sluggish turnover frequency and its sluggish protonolytic activation of precatalysts **1** and **2** at 60 $^{\circ}C$ (typically instantaneous at -78 $^{\circ}C$ in C_7D_8). Also note that the **25** \rightarrow **26** conversion proceeds at turnover frequencies ($N_t = 80 h^{-1}$, An = Th; $N_t = 120 h^{-1}$, An = U; Table 4, entries 9 and 10) far greater than those for analogous 1 $^{\circ}$ aminoalkyne **39** at 25 $^{\circ}C$ (vide infra).

The scope of organoactinide-mediated 1,2-disubstituted (internal) aminoalkene HA/cyclization was also investigated (Table 5). These transformations are most efficient for “activated” styrene conversion **27** \rightarrow **28**, where (CGC)An< precatalysts **1** and **2** effect cyclization under mild conditions with reasonable efficiency ($N_t = 1.3 h^{-1}$, An = Th; $N_t = 0.9 h^{-1}$, An = U; entries 1 and 2). Ancillary ligation effects on the HA/cyclization were also explored, with significantly lower turnover frequencies observed when more coordinatively saturated Me₂SiCp'')₂An< and Cp'')₂An< precatalysts **3–6** were used (Table 5, entries 1–6). At 100 $^{\circ}C$, *ansa*-metallocenes **3** and **4** afford **28** at reasonable rates ($N_t = 5.8$ and $7.0 h^{-1}$ for **3** and **4**, respectively; entries 3

Table 4. Organoactinide-Catalyzed HA/Cyclization of Secondary Amine Substrates Tethered to Alkene and Alkyne C–C Un saturations. Comparison of N_t as a Function of Metal Ionic Radius in C_6D_6

Entry	Substrate	Product ^a	Precatalyst	N_t , h ⁻¹ (°C) ^b
1.			(CGC)Th(NMe ₂) ₂	12 (25)
2.			(CGC)U(NMe ₂) ₂	1.5 (25)
3.			(CGC)Th(NMe ₂) ₂	0.1 (100)
4.			(CGC)U(NMe ₂) ₂	0.1 (100)
5.			(CGC)Th(NMe ₂) ₂	0.5 (60)
6.			(CGC)U(NMe ₂) ₂	0.9 (60)
7.			(CGC)Th(NMe ₂) ₂	0.1 (100)
8.			(CGC)U(NMe ₂) ₂	0.1 (100)
9.			(CGC)Th(NMe ₂) ₂	80 (25)
10.			(CGC)U(NMe ₂) ₂	120 (25)

^a Yields $\geq 95\%$ by ¹H NMR spectroscopy. ^b Determined by ¹H NMR spectroscopy.

Table 5. Organoactinide-Mediated HA/Cyclization of 1,2-Disubstituted Aminoalkene Substrates in C_6D_6 Catalyzed by **1–6**. Comparison of N_t as a Function of Metal Ionic Radius and Ancillary Ligand Environment in C_6D_6

Entry	Substrate	Product ^a	Precatalyst	N_t , h ⁻¹ (°C) ^b
1.			(CGC)Th(NMe ₂) ₂	1.3 (60)
2.			(CGC)U(NMe ₂) ₂	0.9 (60)
3.			(Me ₂ SiCp'') ₂ ThR ₂	5.8 (100)
4.			(Me ₂ SiCp'') ₂ UBn ₂	7.0 (100)
5.			Cp'₂ThR₂	0.2 (100) ^c
6.			Cp'₂UR₂	0.5 (100)
7.			(CGC)Th(NMe ₂) ₂	0.6 (100)
8.			(CGC)U(NMe ₂) ₂	0.2 (100)
9.			(CGC)Th(NMe ₂) ₂	0.2 (100)
10.			(CGC)U(NMe ₂) ₂	2.2 (100)

^a Yields $\geq 90\%$ by ¹H NMR spectroscopy. ^b Determined by ¹H NMR spectroscopy. ^c Polymeric byproduct precipitate observed. Single product detected in solution by ¹H NMR spectroscopy and GC/MS.

and 4), whereas unbridged actinocenes are sluggish ($N_t = 0.2$ and 0.5 h⁻¹ for **5** and **6**, respectively; entries 5 and 6). With unactivated substrates, transformations **29**→**30** and **31**→**32** proceed only at elevated temperatures (100 °C). Pyrrolidine product **30** is obtained with similar N_t values for both **1** and **2** ($N_t = 0.6$ h⁻¹, An = Th; $N_t = 0.2$ h⁻¹, An = U; Table 5, entries 7 and 8), while piperidine **32** formation proceeds with similar efficiency for **1** ($N_t = 0.2$ h⁻¹, An = Th; Table 5, entry 9). As for transformation **15**→**16**, precatalyst **2** mediates **31**→**32** ($N_t = 2.2$ h⁻¹, An = U; Table 5, entry 10) with far greater efficiency

Table 6. HA/Cyclization Results with Aminoalkyne Substrates Mediated by Organoactinide Precatalysts **1–6** in C_6D_6

Entry	Substrate	Product ^a	Precatalyst	N_t , h ⁻¹ (°C) ^b
1.			(CGC)Th(NR ₂) ₂	82 (25)
2.			(CGC)U(NR ₂) ₂	3000 (25)
3.			(Me ₂ SiCp'') ₂ ThR ₂	149 (60)
4.			(Me ₂ SiCp'') ₂ UBn ₂	9.8 (60)
5.			Cp'₂ThR₂	190 (60)
6.			Cp'₂UR₂	15.8 (60)
7.			(CGC)Th(NR ₂) ₂	7.8 (25)
8.			(CGC)U(NR ₂) ₂	1210 (25)
9.			Cp'₂UMe ₂	26 (25)
10.			(CGC)Th(NR ₂) ₂	2.2 (25)
11.			(CGC)U(NR ₂) ₂	170 (25)
12.			(CGC)Th(NR ₂) ₂	4.3 (25)
13.			(CGC)U(NR ₂) ₂	51 (25)
14.			Cp'₂ThMe ₂	0.8 (60)
15.			(CGC)Th(NR ₂) ₂	1.4 (60)
16.			(CGC)U(NR ₂) ₂	5.0 (60)

^a Yields $\geq 95\%$ by ¹H NMR spectroscopy and GC/MS. ^b Determined by ¹H NMR spectroscopy.

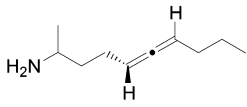
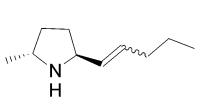
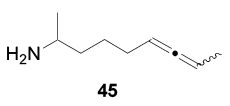
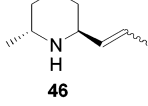
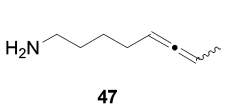
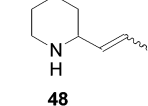
than **29**→**30**, in accord with (CGC)U⟨ catalyst–substrate specificity effects observed with geminal dimethylpiperidine formation (Table 2, entries 9–12; vide infra).

Representative terminal aminoalkene conversion **17**→**18**, mediated by Th catalyst **1**, was examined over a broad temperature range, and from Eyring and Arrhenius analyses,²⁰ $\Delta H^\ddagger = 12.6(5)$ kcal/mol, $\Delta S^\ddagger = -30(1)$ eu, and $E_a = 13.3(7)$ kcal/mol are obtained from 25 to 82 °C. For comparison with internal aminoalkene substrates, the **27**→**28** HA/cyclization promoted by precatalyst **2** was similarly investigated²⁰ between 44 and 84 °C, affording $\Delta H^\ddagger = 16(2)$ kcal/mol, $\Delta S^\ddagger = -28(7)$ eu, and $E_a = 17(2)$ kcal/mol (Table 9).

(b) Aminoalkynes. Terminal and 1,2-disubstituted (internal) aminoalkyne HA/cyclization is effectively mediated by organoactinide complexes **1–6**. As for organo-4f-element catalysts,^{2d,3n,s} this transformation is efficient and highly regioselective at room temperature. The scope of the present aminoalkyne HA/cyclizations includes five- and six-membered ring formation. Conversion **33**→**34** was examined with precatalysts **1–6** to explore the effects of ligand environment (Table 6, entries 1–6). The (CGC)An⟨ framework is by far the most efficient in mediating this transformation, proceeding rapidly at 25 °C ($N_t = 82$ h⁻¹, An = Th; $N_t = 3000$ h⁻¹, An = U; Table 6, entries 1 and 2). Interestingly, in the case of more coordinatively saturated precatalysts **3–6**, N_t at 60 °C increases with decreasing steric openness ($N_t = 149$ h⁻¹, **3**; $N_t = 190$ h⁻¹, **5**; $N_t = 9.8$ h⁻¹, **4**; $N_t = 15.8$ h⁻¹, **6**; Table 6, entries 3–6), although not for (CGC)An⟨ catalysts **1** and **2**. Additionally, the superiority of the (CGC)An⟨ catalyst framework over Cp'₂An⟨ is evident for substrates **35** (An = U; Table 6, entries 8 and 9) and **39**

(20) Espenson, J. H. *Chemical Kinetics and Reaction Mechanisms*, 2nd ed.; McGraw-Hill, Inc.: New York, 1995.

Table 7. HA/Cyclization Results with Aminoallene Substrates in C₆D₆ Mediated by Organoactinide Precatalysts 1–6

Entry	Substrate	Product ^a	Precatalyst	<i>trans</i> : <i>cis</i> ^b	<i>N</i> _t , h ⁻¹ (°C) ^c
1.			(CGC)Th(NMe ₂) ₂	90:10	2.7 (25)
2.			(CGC)U(NMe ₂) ₂	80:20	29 (25)
3.			(Me ₂ SiCp ^{''}) ₂ ThR ₂	60:40	0.03 (25)
4.			(Me ₂ SiCp ^{''}) ₂ UBn ₂	60:40	0.3 (25)
5.	43	44	Cp ^{''} ₂ ThR ₂	70:30	0.3 (100) ^d
6.			Cp ^{''} ₂ UR ₂	65:35	0.8 (100)
7.			(CGC)Th(NMe ₂) ₂	60:40	0.1 (60)
8.			(CGC)U(NMe ₂) ₂	75:25	1.3 (60)
9.					
10.			(CGC)Th(NMe ₂) ₂		0.01 (60)
				(CGC)U(NMe ₂) ₂	

^a Yields $\geq 95\%$ by ¹H NMR spectroscopy and GC/MS. ^b Determined by ¹H NMR spectroscopy. ^c Determined in situ by ¹H NMR spectroscopy. ^d Byproduct precipitate observed. Single set of isomers detected in solution by ¹H NMR spectroscopy.

(An = Th; Table 6, entries 12 and 14), where (CGC)An(*N*_t values are far greater.

The scope of organoactinide-mediated aminoalkyne HA/cyclization and An⁴⁺ ionic radius effects is summarized in Table 6. As noted above, conversion of Me₃Si-substituted **33** is most efficient for both An = Th and U, likely owing to -SiMe₃ group transition-state electronic stabilization (vide infra). Unsubstituted terminal alkyne **35** is rapidly cyclized/tautomerized to **36**, especially by **2**, where *N*_t is ca. 10³ × greater than that for **1** (*N*_t = 7.8 h⁻¹, An = Th; *N*_t = 1210 h⁻¹, An = U at 25 °C; Table 6, entries 7 and 8). More sterically demanding **37**–**38** conversion (Table 6, entries 10 and 11) proceeds rapidly, although with considerably less efficiency with **1** than with **2** (nearly 100×), clearly indicating finely controlled steric and electronic requirements. Electronically assisted transformation **39**→**40** (vide infra) exhibits decreased *N*_t vs that of sterically less-encumbered substrates **35** and **37** for **2** but, for precatalyst **1**, only vs **35** (*N*_t = 4.3 h⁻¹, An = Th; *N*_t = 51 h⁻¹, An = U at 25 °C; Table 6, entries 12 and 13). The relative rates of aminoalkyne HA/cyclization vary differently for **1** and **2**, with -SiMe₃ > -H > -Ph > -Me for An = Th, and -SiMe₃ > -H ≫ -Me > -Ph for An = U. The HA/cyclization of **41**, yielding benzyl-substituted tetrahydropyridine **42**, proceeds less efficiently, requiring higher temperatures (*N*_t = 1.4 h⁻¹, An = Th; *N*_t = 5.0 h⁻¹, An = U at 60 °C; Table 6, entries 15 and 16). As observed with aminoalkenes, metal ionic radius effects diminish considerably in closures to larger-ring products. Plots of [substrate]:[An] vs time (e.g., Figure 3) again exhibit deviations from linearity at low [substrate], which is attributed to product inhibition^{2d} at high conversion. Additionally, representative transformation **37**→**38**, mediated by Th complex **1**, was examined over a 50 °C temperature window to yield²⁰ Δ*H*[‡] = 14(2) kcal/mol, Δ*S*[‡] = -27(5) eu, and *E*_a = 15(2) kcal/mol (Table 9).

(c) Aminoallenes. Intramolecular HA/cyclization of 1,3-disubstituted (internal) aminoallenes is mediated with high regioselectivity by (CGC)An(*N*_t complexes. As for organo-4f-

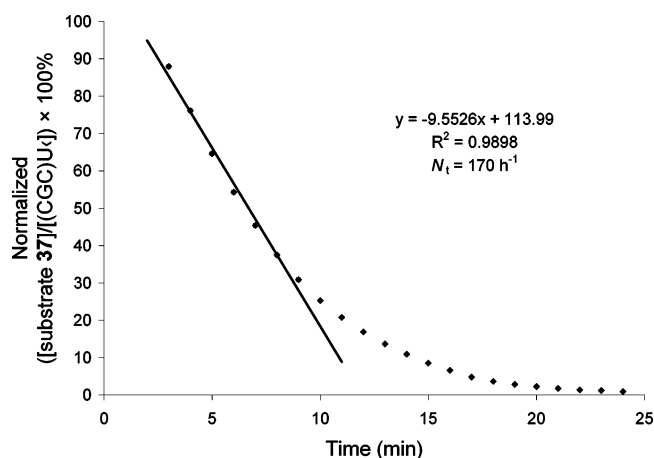


Figure 3. Plot of the normalized ([aminoalkyne **37**]/[(CGC)U]) ratio × 100% ([CGC)U] from precatalyst **2** relative to Si(*p*-tolyl)₄ internal standard) at 25 °C in C₆D₆. The line depicts the least-squares fit, and *N*_t is determined from the slope of the line according to eqs 1 and 2.

element catalysts,^{2d,3h,i,k} such transformations are efficient, highly regioselective, and moderately to highly diastereoselective. The scope of aminoallene HA/cyclization was explored for both five- and six-membered ring products (Table 7). Cyclization of internal aminoallenes **43**, **45**, and **47** proceeds with >90% regioselectivity in forming smaller-ring pyrrolidine or piperidine (kinetically favored) products **44**, **46**, and **48**, with 60–90% *trans*-selective product diastereoselectivities (Table 7, entries 1–8). For conversion **43**→**44**, the effect of ancillary ligand openness on both *N*_t and diastereoselectivity was explored for precatalysts **1**–**6**. Selectivity for *trans* product **44** is comparable for either An = Th or U, regardless of ancillary ligation, although selectivity falls noticeably from (CGC)An(*N*_t to more congested Me₂SiCp^{''}₂An(*N*_t and Cp^{''}₂An(*N*_t frameworks (90:10 *trans*:*cis*, **1**; 80:20, **2**; 60:40, **3** and **4**; 70:30, **5**; 65:35, **6**; Table 7, entries 1–6). The rate of this transformation varies far more upon opening or closing the actinide coordination geometry, with precatalyst **2** exhibiting superior activity vs **4** and **6**, which

Table 8. HA/Cyclization Results with Aminodiene Substrates in C₆D₆ Promoted by Organoactinide Precatalysts 1–6

Entry	Substrate	Products ^a	Precatalyst	Product Ratio ^b	N_t , h ⁻¹ (°C) ^c
1.			(CGC)Th(NMe ₂) ₂	98:2	3.0 (60)
2.			(CGC)U(NMe ₂) ₂	93:7	5.5 (60)
3.			(Me ₂ SiCp ⁺) ₂ ThR ₂	71:29	1.9 (60)
4.			(Me ₂ SiCp ⁺) ₂ UBh ₂	15:85	0.8 (60)
5.			Cp ⁺ ₂ ThR ₂	76:24	0.2 (80)
6.			Cp ⁺ ₂ UR ₂	35:65	0.2 (80)
7.			(CGC)Th(NMe ₂) ₂	93:7	6.1 (60)
8.			(CGC)U(NMe ₂) ₂	81:19	19.9 (60)
9.			(CGC)Th(NMe ₂) ₂	69:31	0.02 (60)
10.			(CGC)U(NMe ₂) ₂	79:21	0.3 (60)

^a Yields \geq 95% by ¹H NMR spectroscopy and GC/MS. ^b Determined by ¹H NMR spectroscopy. ^c Determined in situ by ¹H NMR spectroscopy.

Table 9. Summary of Organolanthanide- and Organoactinide-Mediated HA/Cyclization Activation Parameters Calculated from Standard Eyring and Arrhenius Analyses^a

Unsaturation	Est. ΔH_{rxn} (kcal/mol)		Precatalyst	Substrate	ΔH^\ddagger (kcal/mol)	ΔS^\ddagger (eu)	E_a (kcal/mol)
	step (i)	step (ii)					
aminoalkene	0	-13	Cp ⁺ ₂ La[CH(SiMe ₃) ₂] ^{3v}	9	12.7(5)	-27(2)	13.4(5)
			(CGC)Th(NMe ₂) ₂	17	12.6(5)	-30(1)	13.3(7)
disubstituted aminoalkene	-6	-7	Cp ⁺ ₂ La[CH(SiMe ₃) ₂] ^{3c}	29	18(2)	-25(5)	18(2)
			(CGC)U(NMe ₂) ₂	27	16(2)	-28(7)	17(2)
aminoalkyne	-35	0	Cp ⁺ ₂ Sm[CH(SiMe ₃) ₂] ^{3o}	35	11(8)	-27(6)	--
			(CGC)Th(NMe ₂) ₂	37	14(2)	-27(5)	15(2)
aminoallene	-29	0	Cp ⁺ ₂ LuCH(SiMe ₃) ₂] ^{3j}		17(1)	-16(4)	18(1)
			(CGC)Th(NMe ₂) ₂		43	13(2)	-29(6)
aminodiene	-19	+4/+7	Cp ⁺ ₂ LaCH(SiMe ₃) ₂] ^{3d}	49	10.4(4)	-33(1)	10.4(4)
			(CGC)U(NMe ₂) ₂	49	19(3)	-16(9)	19(3)

^a Data were obtained using Cp⁺₂Ln[CH(SiMe₃)₂] (Ln = La, Sm, Lu) and **1** or **2** as noted over a 40–55 °C temperature range in C₆D₆ for each class of C–C unsaturation. The columns listed as step (i), C–C insertion into M–N bond, and step (ii), protonolysis of cyclized substrate, refer to the proposed mechanism depicted in Scheme 2.

require 100 °C reaction temperatures for moderate rates (N_t = 29 h⁻¹, **2**, 25 °C; N_t = 0.3 h⁻¹, **4**, 25 °C; N_t = 0.8 h⁻¹, **6**, 100 °C; Table 7, entries 2, 4, and 6). A similar trend is evident for An = Th, where precatalyst **1** is far more efficient than either **3** or **5** (N_t = 2.7 h⁻¹, **1**, 25 °C; N_t = 0.03 h⁻¹, **4**, 25 °C; N_t = 0.3 h⁻¹, **5**, 100 °C; Table 7, entries 1, 3, and 5).

The effect of An⁴⁺ ionic radius on rate and selectivity was also investigated for (CGC)An<-promoted aminoallene HA/cyclization reactions (Table 7, entries 1, 2, 7–10). The aforementioned **43**→**44** conversion proceeds smoothly at 25 °C when mediated by either **1** or **2**, although ca. 10× more efficiently for An = U (N_t = 2.7 h⁻¹, An = Th; N_t = 29 h⁻¹, An = U; Table 7, entries 1 and 2). Diastereoselectivities here are comparable, with **1** displaying slightly greater selectivity (90:10 *trans:cis* vs 80:20). In the case of cyclization to piperidine

46, diastereoselectivities are again similar, but **2** exhibits somewhat greater selectivity at 60 °C (75:25 *trans:cis* vs 60:40; Table 8, entries 7 and 8). Furthermore, ca. 10× rate enhancement is again observed for An = U vs An = Th, while for **47**→**48**, precatalysts **1** and **2** effect sluggish conversion for this aminoallene substrate at 100 °C (N_t = 0.01 h⁻¹, An = Th; N_t = 0.1 h⁻¹, An = U; Table 7, entries 9 and 10). Activation parameters for the present aminoallene HA/cyclizations were quantified for representative transformation **43**→**44** mediated by Th complex **1** between 25 and 68 °C. From Eyring and Arrhenius analyses,²⁰ ΔH^\ddagger = 13(2) kcal/mol, ΔS^\ddagger = -29(6) eu, and E_a = 14(2) kcal/mol (Table 9).

(d) Aminodienes. Intramolecular HA/cyclization of terminal and 1,4-disubstituted aminodienes is effectively mediated by (CGC)An< complexes. As for organo-4f-element catalysts,^{2d,3c,f}

such transformations are efficient and exhibit moderate/high regioselectivity at moderate temperatures. The scope spans pyrrolidine and piperidine skeletons, with products evidencing mixed regioselectivities (Table 8), where rate and selectivity vary with actinide identity. Complexes **1** and **2** mediate conversion of aminodiene **49** to allylpyrrolidine **50a**, along with small quantities of (1-propenyl)pyrrolidine byproduct **50b** ($N_t = 3.0 \text{ h}^{-1}$, 98:2 **a:b**, An = Th; $N_t = 5.5 \text{ h}^{-1}$, 93:7 **a:b**, An = U; Table 8, entries 1 and 2). Cyclization **51**→**52a/b** is highly regioselective when promoted by **1** and proceeds more rapidly than **49**→**50a/b** at 60 °C, owing to the geminal dimethyl substitution (Table 8, entry 7). As with substrates having similar structural characteristics (**15** and **31**, vide infra), this transformation is considerably more rapid than that with An = Th or with **2** in the **49**→**50a/b** conversion ($N_t = 19.9 \text{ h}^{-1}$, 81:19 **a:b**, An = U at 60 °C; Table 8, entry 8). Conversion of styrenic substrate **53** to pyrrolidines **54a** and **54b** proceeds with considerably lower N_t values vs that of substrates **49** and **51**, as well as with diminished regioselectivity ($N_t = 0.02 \text{ h}^{-1}$, 69:31 **a:b**, An = Th; $N_t = 0.3 \text{ h}^{-1}$, 79:21 **a:b**, An = U; Table 8, entries 9 and 10).

The influence of actinide ancillary ligation was also investigated for aminodiene HA/cyclization (Table 8, entries 1–6). Both *ansa*-metallocene $\text{Me}_2\text{SiCp}''_2\text{Th}$ (**3**) and unbridged $\text{Cp}''_2\text{Th}$ (**5**) promote the transformation **49**→**50a/b** with moderate regioselectivity (71:29 **a:b**, **3**; 76:24 **a:b**, **5**; Table 8, entries 3 and 5), whereas the An = U congeners exhibit moderate but *opposing* regioselectivity (15:85 **a:b**, **4**; 35:65 **a:b**, **6**; Table 8, entries 4 and 6). Regarding conversion rates, note that the $\text{Cp}''_2\text{An}$ catalysts require 80 °C to achieve sluggish activity, in contrast to the more open organoactinide catalysts ($N_t = 0.2 \text{ h}^{-1}$, An = Th and U; Table 8, entries 5 and 6). While similar steric concerns may be an issue for $\text{Me}_2\text{SiCp}''_2\text{U}$ -mediated formation of **50**, N_t values are comparable for both **3** and **4** ($N_t = 1.9 \text{ h}^{-1}$, An = Th; $N_t = 0.8 \text{ h}^{-1}$, An = U; Table 8, entries 3 and 4). Activation parameters for representative aminodiene HA/cyclization **49**→**50a/b** promoted by complex **2** are $\Delta H^\ddagger = 19$ (3) kcal/mol, $\Delta S^\ddagger = -16$ (9) eu, and $E_a = 19$ (3) kcal/mol between 40 and 82 °C.²⁰ Activation parameters for all organoactinide-catalyzed intramolecular HA/cyclization reactions are summarized in Table 9.

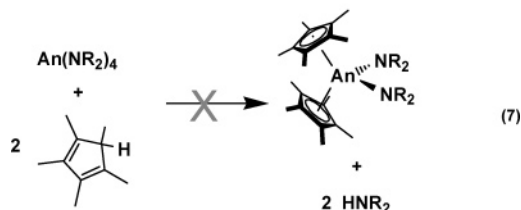
Discussion

We first discuss synthetic and characterization aspects of $(\text{CGC})\text{An}(\text{NMe}_2)_2$ chemistry relating to catalytic intramolecular HA/cyclization reactivity and selectivity. The significance of metal ionic radius and ancillary ligation for catalysis is discussed. Reactivity trends for intramolecular C–N bond-forming processes are analyzed, along with basic mechanistic insights and comparisons with transformations mediated by organo-4f-element and organo-transition metal catalysts. A detailed mechanistic analysis of $(\text{CGC})\text{An}$ -mediated intramolecular HA reactions will be presented in a companion contribution.¹⁶

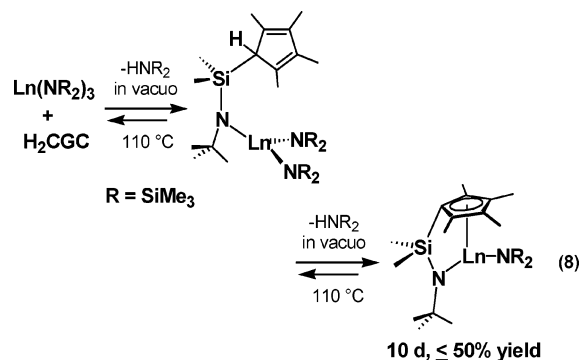
Precatalyst Synthesis and Characterization. Protodeamination routes to d- and f-block metal complexes avoid coordinating solvents and undesired “ate” byproducts.²¹ For example,

(21) (a) Berthet, J. C.; Ephritikhine, M. *Coord. Chem. Rev.* **1998**, *178*–180, 83–116. (b) Kuhlman, R. *Coord. Chem. Rev.* **1997**, *167*, 205–232. (c) Bradley, D. C.; Chisholm, M. H. *Acc. Chem. Res.* **1976**, *9*, 273–280.

$\text{Cp}''_2\text{An}(\text{NR}_2)_2$ actinocenes have been prepared in this manner from the corresponding homoleptic $\text{An}(\text{NR}_2)_4$ reagents and excess HCP (eq 6).^{17,22,23} However, activation of more encumbered rings (e.g., HCp'') has been less successful, even at elevated temperatures, presumably reflecting unfavorable steric interactions and diminished Brønsted acidity (eq 7).²⁴ For the



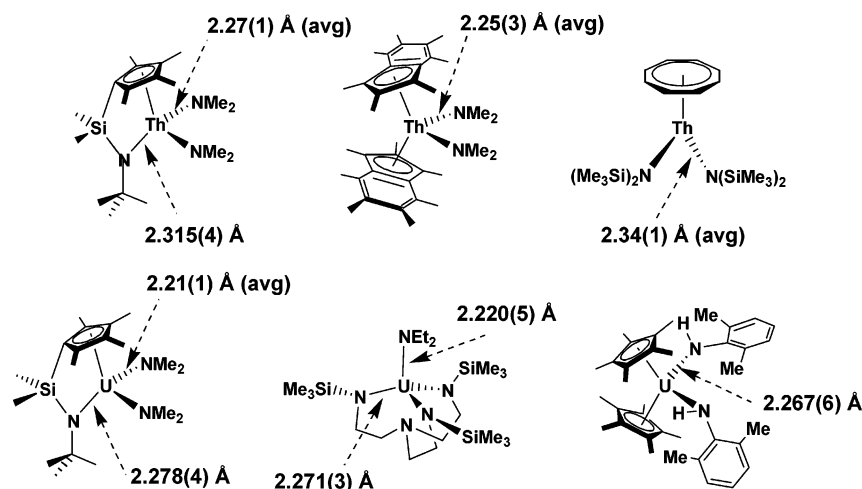
present H_2CGC proligand, HCp'' steric bulk is partially offset by chelation in the final complex.¹³ Interestingly, in the synthesis of $(\text{CGC})\text{Ln}-\text{N}(\text{SiMe}_3)_2$ organolanthanides (Ln = Nd, Sm, Yb, Lu), initial $\text{HN}(\text{SiMe}_3)_2$ displacement and concomitant ligand binding are found to proceed via the $\text{HN}(\text{tBu})$ moiety,^{3j} likely reflecting unfavorable steric interactions (eq 8). The HCp'' group subsequently coordinates via a second protodeamination, both requiring prolonged reflux and $\text{HN}(\text{SiMe}_3)_2$ byproduct removal in vacuo.



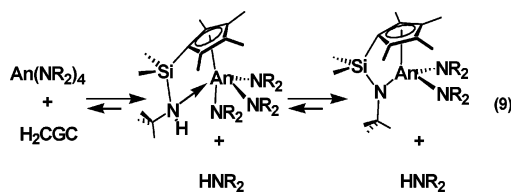
Constrained geometry organoactinide complexes **1** and **2** are conveniently prepared in good yield and high purity from AnCl_4 via one-pot in situ generation of the corresponding tetrakis(dialkylamide) reagents, followed by addition of the H_2CGC proligand (eq 3). In earlier $(\text{CGC})\text{An}(\text{NRR}')_2$ work,¹⁵ similar results were obtained using sublimed, isolated homoleptic amidoactinides. Likewise, LiCl byproduct removal and isolation

- (22) (a) Bagnall, K. W.; Yanir, E. *J. Inorg. Nucl. Chem.* **1974**, *36*, 777–779. (b) Watt, G. W.; Gadd, K. F. *Inorg. Nucl. Chem. Lett.* **1973**, *9*, 203–205. (23) (a) Ossola, F.; Rossetto, G.; Zanella, P.; Arudini, A.; Jamerson, J. D.; Takats, J.; Dormond, A. *Inorg. Synth.* **1992**, *29*, 234–238. (b) Arduini, A. L.; Takats, J. *Inorg. Chem.* **1981**, *20*, 2480–2485. (c) Arduini, A. L.; Jamerson, J. D.; Takats, J. *Inorg. Chem.* **1981**, *20*, 2474–2479. (d) Arduini, A. L.; Edelstein, M.; Jamerson, J. D.; Reynolds, J. G.; Schimid, K.; Takats, J. *Inorg. Chem.* **1981**, *20*, 2470–2474. (e) Jamerson, J. D.; Takats, J. *J. Organomet. Chem.* **1974**, *78*, C23–C25. (f) Jones, R. G.; Karmas, G.; Martin, G. A., Jr.; Gilman, H. *J. Am. Chem. Soc.* **1956**, *78*, 4285–4286. (24) (a) Taft, R. W.; Bordwell, F. G. *Acc. Chem. Res.* **1988**, *21*, 463–469. (b) Bordwell, F. G. *Acc. Chem. Res.* **1988**, *21*, 456–463. (c) Bordwell, F. G.; Bausch, M. J. *J. Am. Chem. Soc.* **1983**, *105*, 6188–6189.

Chart 1



of the crude “An(NR₂)₄” prior to reaction with H₂CGC are equally successful (see Experimental Section for **1**). NMR-scale syntheses, monitored in situ, indicate that crude or pure An(NR₂)₄ protonolysis with H₂CGC is essentially quantitative in benzene-*d*₆ and that appreciable (CGC)An(NR₂)₂ solubility in hydrocarbon solvents limits the isolated yields of analytically pure **1** and **2**. The highest yield was obtained for (CGC)U(NEtMe)₂, which presumably combines –NMe₂ compactness with –NEt₂ steric screening (preventing formation of U(NEtMe)₄ “ate” contaminants) to promote crystallization in analytical purity and ca. 80% yield from UCl₄.¹⁵ In all cases, optimized yields are obtained by incorporating a slight H₂CGC excess to counteract ate contaminant formation and to drive the protodeamination equilibrium to the right (eq 9). Contrary to (CGC)Ln–N(SiMe₃)₂ chemistry,^{3j} the order of ligand attachment (determined in situ by ¹H NMR spectroscopy) more closely follows the expected thermodynamic pathway of protonolysis, whereby the more acidic HCp’ moiety (p*K*_a ~24) binds to the An center first, followed by the HN(‘Bu) moiety (p*K*_a ~33), likely owing to the smaller HNR₂ leaving groups employed for the tetravalent actinides.^{21,23} Also note that the rate at which equilibrium is reached parallels the byproduct amine volatility (rate: HNMe₂, bp 7 °C ≫ HNEtMe, bp 36 °C > HNEt₂, bp 55 °C).



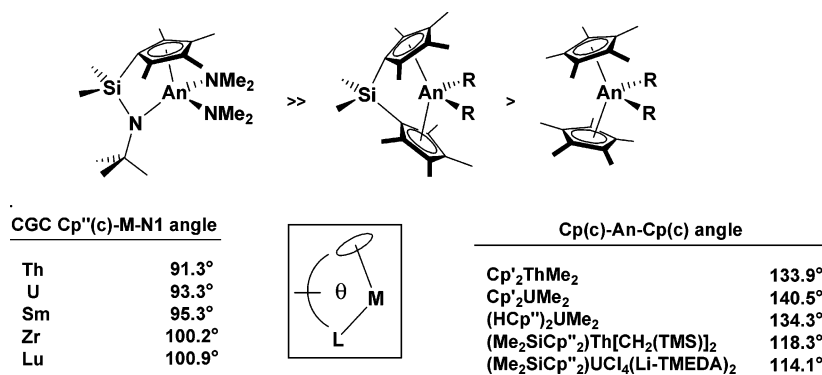
In the case of complexes **1** and **2** (An = Th, U; R = Me), the “An(NR₂)₄” species most likely contain some “ate” contamination, e.g., Li[An(NMe₂)₅],^{17,21–23} resulting from insufficient –NMe₂ group steric screening. This leads to small amounts of byproduct tentatively formulated as Li₂[Me₂Si(η⁵-Me₄C₅)(‘BuN)], which, along with any other pentane-insoluble impurities, is removed by 20 °C filtration prior to –78 °C recrystallization, affording analytically pure (CGC)An(NMe₂)₂ products. The absence of coordinated Lewis bases here allows direct application of **1** and **2** as precatalysts in C–N bond-forming reactions without further purification or undesirable catalytic inhibition.^{3a,u,18}

Single crystals of **1** and **2** suitable for diffraction studies were obtained by slow cooling of saturated pentane solutions. ORTEP depictions of the solid-state structures of **1** and **2** are shown in Figure 1. These complexes display a pseudo-tetrahedral geometry about the An⁴⁺ center, along with a considerably more open coordination environment than that of previously characterized organoactinide complexes (Chart 1). The two An–NMe₂ distances within each complex are nearly identical (within 1σ) and similar to other An–N σ-bonded distances,²⁵ with average An–N bond lengths of 2.27(1) Å (**1**) and 2.21(1) Å (**2**). In comparison, the average Th–N distance of 2.25(3) Å in (η⁵-Me₇C₉)₂Th(NMe₂)₂^{25a} and the U–NEt₂ distance of 2.220(5) Å in (η⁴-[(SiMe₃)NCH₂CH₂]₃N)U(NEt₂)₂^{25b} differ only slightly from those in **1** and **2**, attributable to differences in interligand steric interactions (Chart 1). However, owing to the silyl moiety electron-withdrawing and α-anion stabilization properties,²⁶ in addition to geometric constraints imposed by the ligand structure, the An–N(‘Bu) σ-bond lengths are considerably longer (>3σ) than their An–NR₂ counterparts in both **1** and **2**. This trend is also observed in a series of tetravalent (triamidoamine)-uranium complexes, namely (η⁴-[(SiMe₃)NCH₂CH₂]₃N)U–X (X = Cl, Br, I, NEt₂, or Cp’),^{25b,d} aryl-substituted Cp’₂U[N(H)–Ar]₂ (Ar = 2,6-dimethylphenyl),^{25c} and bis[8]annulene (η⁸-COT)Th[N(SiMe₃)₂]₂^{25e} complexes. Considering the difference in ionic radii between the two metals (Table 1),¹⁰ note that this effect appears to be less pronounced in the Th–N(‘Bu) bond length in **1** vs the U–N(‘Bu) distance in **2**, perhaps a consequence of geometric constraints imposed by the chelating CGC^{2–} ligand. The Cp’ rings in **1** and **2** are coordinated to the respective actinide centers in an η⁵ manner, as indicated by the C–C bond lengths and Cp’’(c)–An distances, without evidence for significant η⁵→η³ ring-slippage²⁷ (Figure 1).

Compared with previously characterized organoactinide complexes bearing similar ancillary ligation,²⁸ the solid-state structures of **1** and **2** indicate considerably greater metal center steric openness/coordinative unsaturation (Chart 2). The Cp–

- (25) (a) Trnka, T. M.; Bonanno, J. B.; Bridgewater, B. M.; Parkin, G. *Organometallics* **2001**, *20*, 3255–3264. (b) Roussel, P.; Alcock, N. W.; Boaretto, R.; Kingsley, A. J.; Munslow, I. J.; Sanders, C. J.; Scott, P. *Inorg. Chem.* **1999**, *38*, 3651–3656. (c) Straub, T.; Frank, W.; Reiss, G. J.; Eisen, M. S. *Dalton Trans.* **1996**, 2541–2546. (d) Scott, P.; Hitchcock, P. B. *Dalton Trans.* **1995**, 603–609. (e) Gilbert, T. M.; Ryan, R. R.; Sattelberger, A. P. *Organometallics* **1988**, *7*, 2514–2518.
- (26) (a) Brinkman, E. A.; Berger, S.; Brauman, J. I. *J. Am. Chem. Soc.* **1994**, *116*, 8304–8310. (b) Hopkinson, A. C.; Lien, M. H. *J. Org. Chem.* **1981**, *46*, 998–1003.

Chart 2

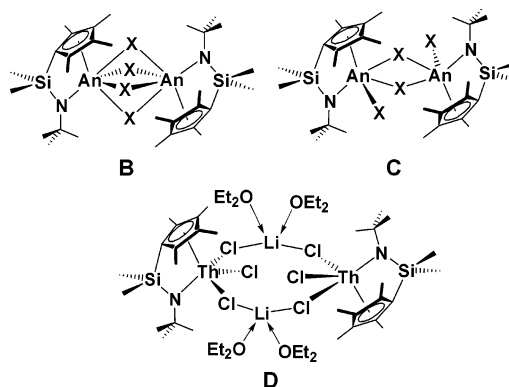


(c)-An-L angles (L = N(^tBu), Cp'', Cp') of 91.3° and 93.3° determined for **1** and **2**, respectively, evidence considerably greater openness vs **3** (118.3°),²⁹ closely related "ate" complex Me₂SiCp''₂U(μ-Cl)₄[Li(TMEDA)]₂ (114.1°),³⁰ (HCp'')₂UMe₂ (134.3°),^{28a} Cp'₂ThMe₂ (133.9°),^{28b} or Cp'₂UMe₂ (140.5°),^{28b} indicating enhanced An center accessibility. The less constrained Me₂SiCp''₂An (**3** and **4**) and Cp'₂An (**5** and **6**) ligand environments are quantifiably less accessible to incoming substrates by ca. 25° and 40°, respectively, vs (CGC)An (**1** and **2**).

Compared to charge-neutral (CGC)Ln-E(SiMe₃)₂ (Ln = Sm, E = N; Ln = Lu, E = CH),^{3j} complexes, the present organoactinide coordinative openness is greater, with larger lanthanide ions displaying Cp(c)-Ln-N(^tBu) angles ranging from 95.3° (Ln = Sm) to 100.9° (Ln = Lu) (Chart 2). This trend can be rationalized in terms of metal ionic radius, where eight- and nine-coordinate ionic radii¹⁰ for selected Ln³⁺ and An⁴⁺ ions are listed in Table 1. Overall, trends in the Cp''(c)-An-N1 angle indicate that the steric openness in f-element CGC complexes increases in the order Lu ≪ Sm < U < Th. Versus related tetravalent group 4 complexes, the considerably less open ∠Cp(c)-M-N(^tBu) of 100.2° in (CGC)Zr(NMe₂)₂,³¹ among other steric and electronic factors, is in accord with the diminished catalytic activity in mediating aminoalkene HA/cyclization.^{2,16}

Analytically pure (CGC)AnX₂ (An = Th, **1-Cl**₂ and **1-I**₂; An = U, **2-Cl**₂ and **2-I**₂) dihalide complexes are prepared in quantitative yield by reaction of **1** or **2** with excess Me₃SiX reagents (eq 4). These complexes are insoluble in non-coordinating solvents and precipitate immediately from solution as fine powders, allowing removal of the byproduct amine in vacuo or by suitable washing. This synthetic strategy is particularly useful for one-pot reactions, proceeding through the dihalides **1-X**₂ and **2-X**₂. Although poor solubility precludes cryoscopic molecular weight determination, the open coordination spheres and frequent observation of d⁰- and f-block bridging

halide complexes^{12,13,19,32} suggests that these complexes may exist as dimers or trimers (vide infra). ¹H NMR studies in THF-d₈ solution are in agreement with a single C_s-symmetric instantaneous species at 20 °C, consistent with formation of a monomeric, fluxional THF adduct or symmetric [(CGC)An(μ-X)₂]₂ (**B**) or [(CGC)AnX(μ-X)]₂ (**C**) structures. Interestingly, while the solubility of these dihalides in THF is typical of organoactinide halides, the solubility of **1-Cl**₂ and **2-Cl**₂ in diethyl ether or hydrocarbons is far less, prompting the synthesis of analogous diiodides **1-I**₂ and **2-I**₂. These display improved solubility in diethyl ether, but not in hydrocarbons.



Closely related [(CGC)ThCl(μ-Cl)₂Li(OEt₂)₂]₂ was prepared in 43% yield via a traditional salt elimination route from ThCl₄ with Li₂CGC in diethyl ether³³ and exhibits solid-state structure **D**, with each Th center retaining an additional chloride ligand. While it is unlikely that catalytic activity would be observed for any of these species without the addition of a cocatalytic reagent (e.g., MAO and/or AlR₃),³⁴ the absence of residual Lewis bases in the coordination spheres of **1-Cl**₂, **2-Cl**₂, **1-I**₂, and **2-I**₂ reduces the possibility of catalyst inhibition. Furthermore, base-free dihalide complexes **1-X**₂ and **2-X**₂ can be obtained from crude, AnCl₄-derived (CGC)An(NR₂)₂ complexes in high overall yield.

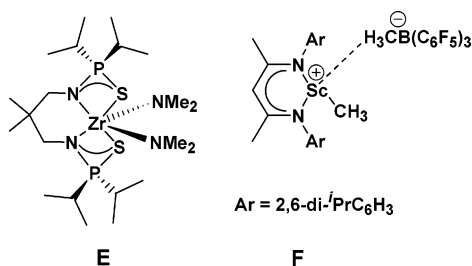
Catalytic C-N Bond Formation. The following discussion focuses on (CGC)An catalytic properties in mediating HA/cyclization of diverse primary and secondary amines, tethered

(27) See, for example: Basolo, F. *New J. Chem.* **1994**, *18*, 19–24.
 (28) (a) Evans, W. J.; Kozimor, S. A.; Hillman, W. R.; Ziller, J. W. *Organometallics* **2005**, *24*, 4676–4683. (b) Jantunen, K. C.; Burns, C. J.; Castro-Rodriguez, I.; Da Re, R. E.; Golden, J. T.; Morris, D. E.; Scott, B. L.; Taw, F. L.; Kiplinger, J. L. *Organometallics* **2004**, *23*, 4682–4692.
 (29) (a) Fendrick, C. M.; Schertz, L. D.; Day, V. W.; Marks, T. J. *Organometallics* **1988**, *7*, 1828–1838. (b) Fendrick, C. M.; Mintz, E. A.; Schertz, L. D.; Marks, T. J. *Organometallics* **1984**, *3*, 819–821.
 (30) Schnabel, R. C.; Scott, B. L.; Smith, W. H.; Burns, C. J. *J. Organomet. Chem.* **1999**, *591*, 14–23.
 (31) Carpenetti, D. W.; Kloppenburg, L.; Kupec, J. T.; Petersen, J. L. *Organometallics* **1996**, *15*, 1572–1581.

(32) See, for example: Fagan, P. J.; Manriquez, J. M.; Marks, T. J.; Day, C. S.; Vollmer, S. H.; Day, V. W. *Organometallics* **1982**, *1*, 170–180 and references therein.
 (33) Golden, J. T.; Kazul'kin, D. N.; Scott, B. L.; Voskoboinikov, A. Z.; Burns, C. J. *Organometallics* **2003**, *22*, 3971–3973.
 (34) For general reviews, see: (a) Barron, A. R. *Metallocene-Based Polyolefins* **2000**, *1*, 33–67. (b) Chen, E. Y.-X.; Marks, T. J. *Chem. Rev.* **2000**, *100*, 1391–1434 and references therein.

to diverse C–C unsaturations. Beginning with simple terminal aminoalkenes and progressing through additional substrate classes, the expansive scope and powerful C–N bond-forming ability of (CGC)An⟨ catalysts are placed in context with relevant literature and likely mechanistic scenarios.

(a) Aminoalkenes. (CGC)An⟨ complexes rapidly and regioselectively mediate intramolecular HA/cyclization of terminal and disubstituted aminoalkenes. Compared to other catalyst systems, the efficacy of precatalysts **1** and **2** is impressive, displaying scope and activity comparable to those of complexes of intermediate-sized Ln³⁺ ions stabilized by similar ligands,^{2d} and the aminoalkene HA/cyclization rates far exceed those of systems mediated by group 4 catalysts, all of which require heating to ≥100 °C and/or Lewis acid activators.^{5d,f,h,i} Rates of organoactinide-catalyzed aminoalkene conversion to the corresponding pyrrolidines and piperidines are highly dependent on ancillary ligation and ionic radius, with complexes that offer greater access to the Ln center being the most active catalysts. For example, the **9**→**10** conversion, promoted by trivalent Cp′₂Ln– catalysts, proceeds more rapidly with larger radius metals, i.e., La (*N_t* = 95 h^{−1}) > Sm (4.8 h^{−1}) > Lu (0.03 h^{−1}) at 25 °C. Expanding the degree of coordinative unsaturation yields a similar trend: (CGC)Lu– (90 h^{−1}) ≫ Me₂Si(Cp′′)–(Cp)Lu– (4.2 h^{−1}) > Me₂SiCp′′₂Lu– (1.6 h^{−1}) > Cp′₂Lu– (0.03 h^{−1}) at 25 °C.^{3i,u,35} Examples of 1° aminoalkene HA/cyclizations mediated by early transition metal complexes are limited, proceeding similarly to those with the aforementioned Ln³⁺, but with far less efficiency (e.g., with Ti(NMe₂)₄^{5d} and chelated diamide **E**).^{5f} Notably, cationic β-diketiminatoscandium complex **F** displays significantly increased catalytic activity vs the neutral LScMe₂ analogue, most likely a consequence of the more accessible, more electrophilic metal center.^{4h} Similar cationic group 4 species mediate HA/cyclization of 2° aminoalkenes, with apparent deactivation by 1° amine substrates (vide infra).^{5h,i}



Reactivity patterns for organoactinide-mediated HA/cyclization of 1° aminoalkenes largely parallel those of other highly electrophilic catalysts, with considerably greater activities than for group 4 catalysts.^{5d,f,h,i} Terminal aminoalkene conversions are efficient and highly regioselective at room temperature, without an induction period,³⁶ exclusively providing exocyclic products. In general, larger, more unsaturated An complexes mediate this transformation most rapidly. Thus, (CGC)An⟨ complexes **1** and **2** are the most active organoactinide catalysts yet discovered, with *N_t* increasing ca. 10× upon proceeding from Cp′₂An⟨ → Me₂SiCp′′₂An⟨ → (CGC)An⟨ (Chart 2). Interestingly, the most abrupt activity increase occurs from Cp′₂An⟨ to Me₂SiCp′′₂An⟨, although the Cp(c)–An–L angles discussed

(35) Where necessary, *N_t* values at 25 °C estimated on the basis of activation parameters determined in the lead reference.

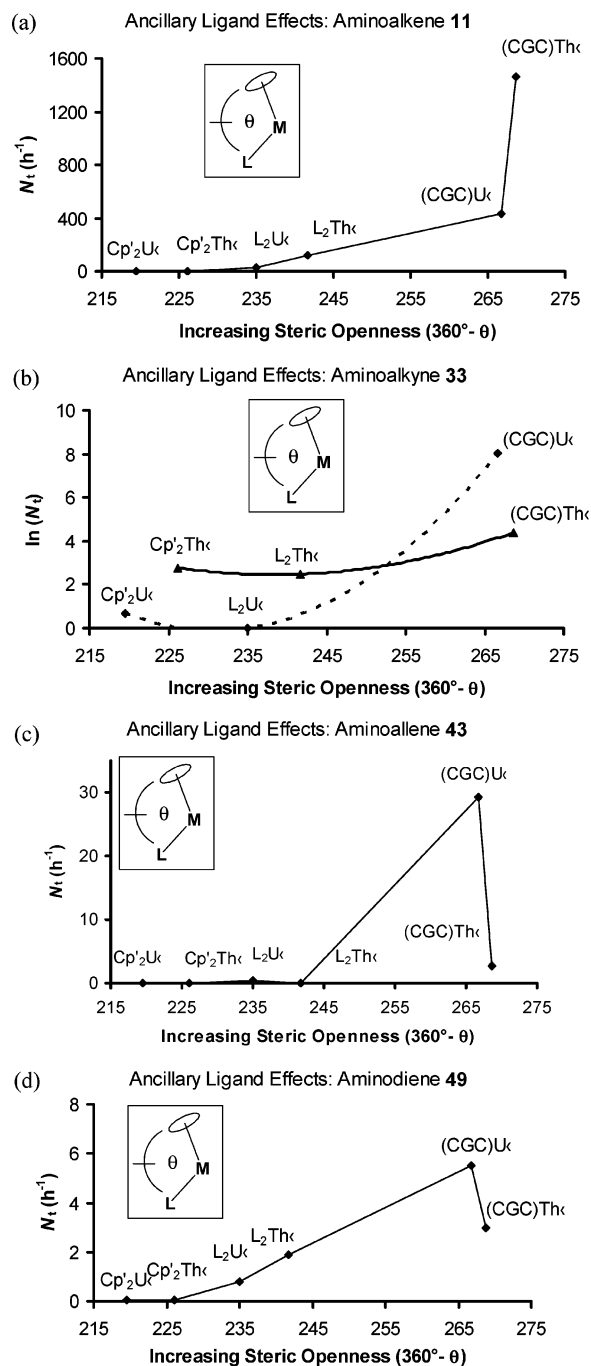
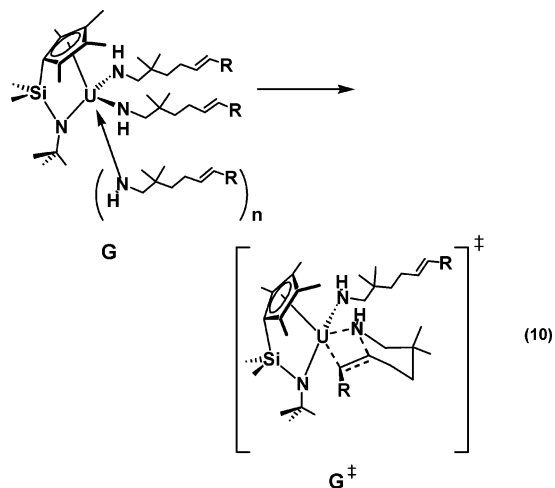


Figure 4. Plots of *N_t* vs increasing steric openness (360° - θ; Chart 2) for intramolecular HA/cyclizations of (a) aminoalkene **11**→**12**, (b) aminoalkyne **33**→**34** (ln(*N_t*) vs increasing openness), (c) aminoallene **43**→**44**, and (d) aminodiene **49**→**50** mediated by the indicated organoactinide complexes **1**–**6** (L₂An⟨ corresponds to **3** and **4**, L₂[−] = [Me₂SiCp′′₂]^{2−}) in C₆D₆ and extrapolated to 25 °C. Curves are drawn as a guide to the eye.

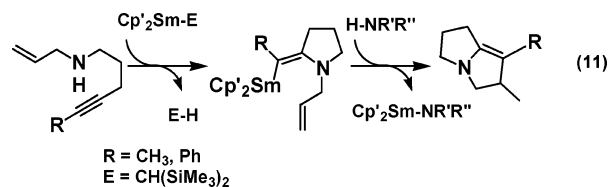
above transition in roughly equal degrees, reflecting a remarkable sensitivity of this transformation to ancillary ligand openness. Nevertheless, the *N_t* increase on proceeding to more open precatalysts **1** and **2** is indeed significant, with greater thermal stability^{29,30,37} than for **3** and **4** and greater access to more demanding transformations (vide infra). This trend in increasing activity with increasing coordinative unsaturation, as indexed by ∠Cp(c)–M–L (Chart 2), is summarized graphically in Figure 4a for **11**→**12**, perhaps approaching an asymptotic limit.

The scope of 1° aminoalkene HA/cyclization was further investigated with **1** and **2** to assess the importance of actinide ionic radius (Tables 1 and 3). Overall, the data for the wide range of substrate structures and substitutions generally parallels 4f trends,^{2d} namely that larger metal centers more rapidly mediate HA/cyclization, geminal dialkyl substitution accelerates cyclizations, and five-membered pyrrolidines form more rapidly than six-membered piperidines. The Thorpe–Ingold effect³⁸ in stabilizing the likely four-centered, insertive transition state (**A**) is pervasive here,^{39,40} typically resulting in 100-fold rate enhancements upon geminal dialkyl substitution, exemplified by substrates **7** vs **9**, **13** vs **15**, and again for **9** vs **11**, **15** vs **17**. Interestingly, this is not the case for the **15**→**16** conversion promoted by **2**, where N_t is *greater* than that for **17**→**18**. Remarkably, **15**→**16** is also considerably more efficient than **9**→**10**, in spite of the five- to six-membered ring size increase, contrary to the Baldwin ring-closure rules.⁴¹ This interesting result is likely a consequence of the finely tuned steric requirements for intramolecular HA/cyclization and is also observed for similar substrates in reactions catalyzed by (CGC)U. Internal alkene **31**→**32** (Table 5) and conjugated 1,3-diene **51**→**52a/b** (Table 8) conversions, where each substrate possesses the same H₂NCH₂C(Me)₂CH₂CH₂– structure adjacent to the C=C fragment, appear to create an almost enzyme-like⁴² “sweet spot” for cyclization (e.g., eq 10).

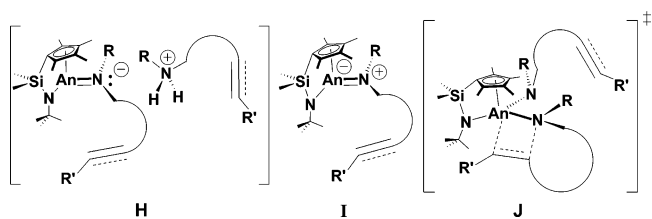


The catalytic addition of 2° N–H bonds across C=C functionality was also explored, with **1** and **2** typifying the ability of more open (CGC)An complexes to mediate more sterically

demanding cyclizations. As expected on the basis of its structural similarity to **9**, simple 1° amine substrate **19** is rapidly converted to **20a** at 25 °C, with strained bicyclic **20b** requiring heating to 100 °C. An identical N_t is observed for **23**→**24** under similar conditions (Table 4), where more hindered *N*-benzyl substitution is combined with reduced *N* nucleophilicity. Less forcing conditions are required for less encumbered *N*-methyl substrates **21** and **25** (Table 4), indicating that steric factors are important, although the An⁴⁺ size dependence suggests that ancillary ligation openness is also important. Note also the rate *enhancement* for **25**→**26** vs analogous *N*-unprotected aminoalkyne **39**→**40** (Tables 5 and 7). In that 2° aminoalkenes present greater steric impediment to cyclization than their *N*-unprotected congeners (see structure **A**), this result is consistent with previously reported rate increases with decreasing Ln³⁺ ionic radius in aminoalkyne HA/cyclization (vide infra).^{3n,s} A similar enhancement in activity is seen in sequential C–N/C–C bond-forming processes mediated by Cp₂Sm– catalysts (eq 11).^{3l} Interestingly, in the case of Cp₂Sm–, alkyne terminus phenyl substitution leads to a *decrease* in cyclization rate, indicative of unfavorable steric interactions during C–C insertion into the M–N bond in transition state **A**.



The competence of **1** and **2** in mediating facile 2° aminoalkene transformations argues against an easily accessible An=NR intermediate/transition state in C–N bond formation (cf. Scheme 3).⁴³ Less plausible high-energy species such as **H** or **I** must be invoked in place of more plausible **J**. Ion pair **H**, presumably

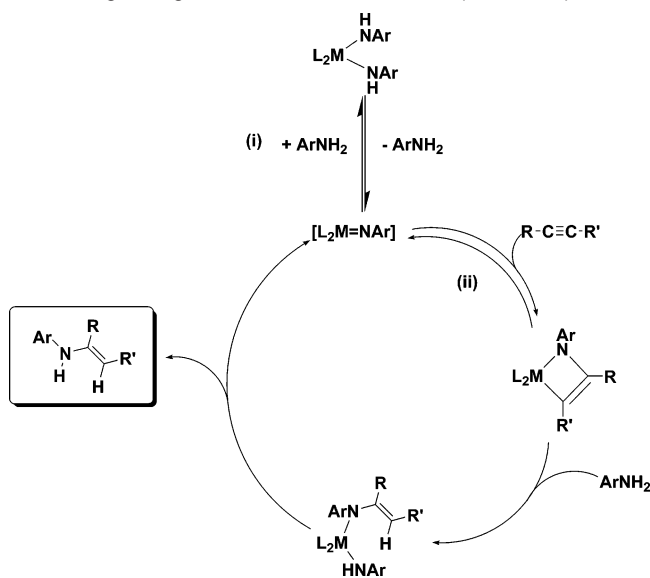


generated via unimolecular α-H⁺ abstraction, features An-coordinated hypervalent N, while zwitterion **I** (by way of N-based electron pair transfer to the An–N bond) places a formal negative charge on electrophilic Th⁴⁺ or U⁴⁺ (no change in ¹H NMR paramagnetic shifts is observed vs similar 1° amine HA/cyclization processes). In regard to possible radical pathways, the high regioselectivity observed for An-mediated cyclizations of 2° aminoalkene and aminoalkyne substrates is inconsistent with radical chain processes.⁴⁴ Additionally, the required but energetically unfavorable An⁴⁺→An³⁺ electron transfer/reduction for An–N(H)R homolysis (particularly for An = Th),^{12,13} the rate dependence on metal ionic radius, the zero-order dependence on [substrate],²⁰ and pronounced effects

- (36) Induction periods have been reported in support of a [2+2] cycloaddition pathway proceeding via a rapid pre-equilibrium for *intermolecular* HA mediated by group 4 and An metals. The proposed active species, L₂M=NR, is postulated to form via α-elimination from L₂M[N(H)R]₂ species (see refs 2a,h–n and 16 for details).
- (37) Stubbert, B. D. Ph.D. Thesis, Northwestern University, 2006. Prolonged reaction times and forcing conditions (*T* > 120 °C) in alkane and aromatic solvents do not induce catalyst decomposition with similar 1° and 2° amine substrates.
- (38) Sammes, P. G.; Weller, D. J. *Synthesis* **1995**, 1205–1222.
- (39) (a) Motta, A.; Fragala, I. L.; Marks, T. J. *Organometallics* **2006**, *25*, 5533–5539. (b) Motta, A.; Lanza, G.; Fragala, I. L.; Marks, T. J. *Organometallics* **2004**, *23*, 4097–4104.
- (40) (a) Tobisch, S. *Dalton Trans.* **2006**, No. 35, 4277–4285. (b) Tobisch, S. *Chem. Eur. J.* **2006**, *12*, 2520–2531. (c) Tobisch, S. *J. Am. Chem. Soc.* **2005**, *127*, 11979–11988.
- (41) March, J. *Advanced Organic Chemistry: Reactions, Mechanisms, and Structure*, 4th ed.; John Wiley & Sons: New York, 1992.
- (42) See, for example: (a) Shakhnovich, E. I. *Nat. Struct. Biol.* **1999**, *6*, 99–102. (b) Stryer, L. *Biochemistry*, 4th ed.; W. H. Freeman and Co.: New York, 1995; pp 181–206.

- (43) Hazari, N.; Mountford, P. *Acc. Chem. Res.* **2005**, *38*, 839–849.
- (44) (a) Walton, J. C.; Studer, A. *Acc. Chem. Res.* **2005**, *38*, 794–802. (b) Kemper, J.; Studer, A. *Angew. Chem., Int. Ed.* **2005**, *44*, 4914–4917. (c) Newcomb, M.; Burchill, M. T.; Deeb, T. M. *J. Am. Chem. Soc.* **1988**, *110*, 6528–6535.

Scheme 3. Proposed [2+2] Cycloaddition Mechanistic Pathway Proceeding through an $L_2M=NAr$ Intermediate ($M = Ti, Zr$)^a

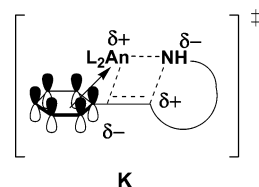


^a This mechanistic scenario is consistent with the observed rate law, $v \sim [L_2M^{4+}]^1[alkyne]^1[amine]^{-1}$, in the *intermolecular* HA of alkynes with bulky (aromatic) amines. A similar pathway is proposed for Cp'_2An^{4+} -mediated processes displaying zero-order dependence on [alkyne] (see refs 2 and 47–50).

of ancillary ligation on N_T and cyclization diastereoselectivity all render radical pathways unlikely, especially in view of the poor regioselectivity and overall yield in radical-mediated aminoalkene cyclizations.^{44b,c} Results for cationic group 4 metal-catalyzed aminoalkene HA/cyclizations, where 1° aminoalkenes deactivate L_2Ti^{+} and L_2Zr^{+} catalysts,^{5h,i} suggest that, in these cases, neutral $L_2M=NR$ imido species are unreactive with respect to $C=C$ insertion (eq 12), unlike the highly reactive intermediate proposed in group 4 *intermolecular* HA.^{2a} Additional experiments probing the detailed mechanism of intramolecular 1° and 2° amine HA/cyclization mediated by (CGC)An \langle and (CGC)Zr \langle catalysts will be reported elsewhere.¹⁶

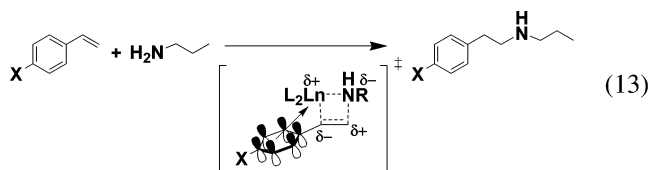


Regarding internal (1,2-disubstituted) aminoalkene HA/cyclizations, trends are similar to those observed for terminal olefinic substrates and those mediated by 4f catalysts.^{2d} Specifically, Th-mediated transformations are generally more rapid than those mediated by U^{4+} , and more open (CGC)An \langle and $Me_2SiCp''_2An\langle$ complexes are more active than $Cp'_2An\langle$ catalysts (Table 5). Specifically, (CGC)An \langle catalysts are $\sim 10\times$ more active than the corresponding $Me_2SiCp''_2An\langle$ catalysts. In the conversion **27**→**28**, it is plausible that the electron-withdrawing phenyl ring stabilizes the δ^- charge in the proposed transition state **K** ($R = Ph$), thereby assisting turnover-limiting $C=C$ insertion, despite unfavorable steric interactions (Table 4).^{3e,12} Additional stabilization may be provided by arene ring π -coordination to the electrophilic $L_2An\langle$ center (**K**). Studies of Ln-mediated *intermolecular* substituted styrene HA invoked a similar pathway to explain the impressive anti-Markovnikov



K

regioselectivity and X effects on rate (eq 13).^{3e} “Unactivated” substrates **29** and **31** are converted to **30** and **32**, respectively, at elevated temperatures (100 °C; Table 5) but otherwise closely follow patterns observed for **9**→**10** and **15**→**16**.

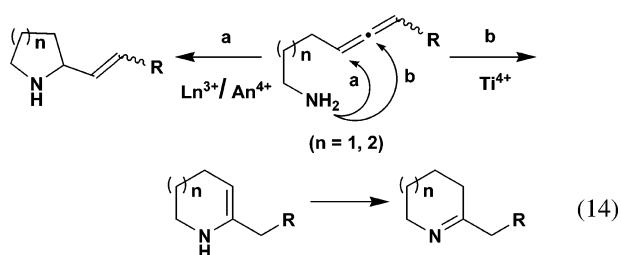


(b) Aminoalkynes. The present (CGC)An \langle complexes rapidly and regioselectively catalyze aminoalkyne HA/cyclization under mild conditions. Previous observations with organolanthanide catalysts indicate extremely high activity for Ln complexes of *smaller* ionic radius.^{3n,s} For example, **35**→**36** conversion is efficiently mediated at 21 °C by Cp'_2Ln-R precatalysts, with the observed relative rates $Lu (5.3) > Sm (4.3) > Nd (1.5) > La (1)$. This trend is paralleled by the ca. $40\times$ fall in activity upon opening the catalyst coordination sphere of Cp'_2Sm-R (77 h^{-1}) to $Me_2SiCp''_2Sm-R$ (2 h^{-1}) in **39**→**40** HA/cyclization, exactly *contrary* to aminoalkene trends.^{2d} Group 4 catalysts also mediate the intramolecular HA/cyclization of highly reactive aminoalkynes, displaying greater reactivity with $M = Ti$ than with $M = Zr$, although electronic considerations and ancillary ligand steric requirements are less clearly defined.^{2a,h-n} Rates with Ti^{4+} complexes (proposed to proceed through a [2+2] cycloaddition pathway, Scheme 3) are, in some cases, comparable to those obtained with Ln^{3+} complexes.²

Consistent with these observations, intramolecular aminoalkyne HA/cyclization mediated by **1** and **2** proceeds rapidly and regioselectively (Table 6). N_T values are comparable to or greater than those of L_2Ln-R catalysts.³ⁿ Thus, conversions **35**→**36** and **37**→**38**, mediated by **2**, proceed at ca. twice the rate of reactions with Cp'_2Sm-R catalysts, establishing **2** as the most efficient catalyst reported for this transformation. While the **2**-mediated conversion **33**→**34** is extremely rapid ($N_T \approx 3000 h^{-1}$, 25 °C), it is even more so when catalyzed by similarly sized L_2Ln-R species.^{3n,s} Regarding transition state **A** and the tendency of Me_3Si- functionalities to stabilize α -carbanions and β -carbocations²⁶ (outweighing steric impediments to $C\equiv C$ insertion), this difference in reactivity may reflect a reduced tendency for An^{4+} (vs Ln^{3+}) ions to stabilize γ -agostic interactions with proximate Si–C bonds.^{12f} Or, considering the presence of a second, covalently bonded substrate moiety, this difference may reflect a balance in steric vs electronic factors in the highly polarized transition state (vide infra). Notably, more electrophilic Th^{4+} appears to favor arene coordination/transition-state stabilization (as discussed above for **27**→**28**) more effectively than U^{4+} , perhaps reflecting differences in 5f-element bond covalency.^{12,13} Moreover, the dispersion in rates with alkyne substitution for **1** ($-SiMe_3 > -H > -Ph > -Me$) vs the more Cp'_2Sm -like³ⁿ behavior of **2** ($-SiMe_3 \gg -H \gg -Me > -Ph$) suggests a complex interplay of sterics and electronics.

Ancillary ligand effects on aminoalkyne HA/cyclization were also investigated with **1–6**. Reactivity patterns largely parallel those of the $\text{Cp}'_2\text{Ln}-$ and $\text{Me}_2\text{SiCp}''_2\text{Ln}-$ systems,³ⁿ with rates following the general trend $\text{Cp}'_2\text{An}\langle > \text{Me}_2\text{SiCp}''_2\text{An}\langle$, and ca. $10\times$ greater activity for the *larger* Th^{4+} center with each ligand set. However, a sharp deviation from this trend is observed with the markedly more open, coordinatively unsaturated (CGC)An \langle catalysts, with relative rates for **33**→**34** of roughly 82 (**1**):12 (**3**):16 (**5**) h^{-1} for An = Th and 3000 (**2**):1 (**4**):2 (**6**) h^{-1} for An = U. This reveals a remarkable increase in catalytic activity ($>10^3$ -fold; Figure 4b) with (CGC)An \langle catalysts and provides a dramatic demonstration of successfully combining the electronic and coordinative unsaturation characteristics of CGC ligation in organometallic catalysis.¹¹

(c) Aminoallenes. Intramolecular (CGC)An \langle -mediated HA/cyclization of 1,3-disubstituted allenes covalently linked to 1° amines proceeds under mild conditions, displaying moderate *trans*-2,5-pyrrolidine and *trans*-2,6-piperidine diastereoselectivity along with $>90\%$ regioselectivity. Compared to similar transformations effected by group 4^{5k,1} and Ln complexes,^{3h,i,k} (CGC)An \langle complexes display comparable activities and activity trends. The scope of such conversions previously investigated with organo-group 3 and 4f catalysts demonstrated impressive, regioselective routes to natural products.^{3h} Mechanistic analysis revealed an unusual dependence on Ln^{3+} ionic radius, with maximum N_i values for intermediate ionic radii, and an “alkyne-like” dependence on catalyst ancillary ligation, with (CGC)Y-catalyzed reactions exhibiting marked diminution of cyclization rates vs $\text{Cp}'_2\text{Y}-$.³ⁱ Furthermore, group 4 catalysts with chelating bis(sulfonamide) ligands (likely providing greater steric openness and electrophilicity) exhibit striking enhancements in activity as well as scope over traditional group 4 metallocenes.^{5k,1} Interestingly, regioselectivities for Ln- and Ti-based processes are reversed, with Ln^{3+} and An^{4+} catalysts selectively generating exocyclic rings (pathway **a**, eq 14) vs formation of endocyclic regioisomers with Ti^{4+} catalysts (pathway **b**, eq 14);^{3i,5k} both pathways are favorable within the Baldwin ring-closure rules.⁴¹ Zr-mediated transformations also operate via pathway **a** and cyclize 1,3,3-trisubstituted aminoallenes in moderate yields and with $>90\%$ regioselectivity, although more sluggishly than those with similarly ligated Ti catalysts.⁵¹



Overall, (CGC)An \langle catalyst selectivity and activity (Table 7) more closely resemble organolanthanide patterns than those of Ti/Zr- catalysts. However, comparing $\text{Me}_2\text{SiCp}''_2\text{An}\langle$ vs $\text{Cp}'_2\text{An}\langle$ coordinative unsaturation, precatalysts **3–6** exhibit sluggish efficiencies and moderate diastereoselectivities, unlike the general trend observed with lanthanocenes (*increasing* reactivity with *decreasing* coordinative unsaturation).³ⁱ Rather the An trend resembles smaller, tetravalent Ti/Zr patterns, suggesting that increased encumbrance introduced by an additional covalent σ -bond may impose greater steric constraints on transition state

A (Scheme 2) and rate-limiting C=C insertion into the An–N bond (cf. **G**, **G**[‡], and **J**). Likewise, the additional bond covalency of An (vs Ln) ions may help stabilize **A**. A qualitative comparison of coordinative unsaturation effects on N_i (according to the $\text{Cp}(c)\text{—M—L}$ angle θ in Chart 2) is presented in Figure 4c for **43**→**44** conversion mediated by precatalysts **1–6**.

More striking are $\text{Me}_2\text{SiCp}''_2\text{An}\langle \rightarrow (\text{CGC})\text{An}\langle$ ancillary ligand effects, where cyclization rates are comparable to those of rapid, $\text{Cp}'_2\text{Ln}$ -promoted reactions.³ⁱ With the exception of the “preorganized” aminoallene **43**, which exhibits a $10\times$ rate enhancement for cyclization mediated by $\text{Cp}'_2\text{Sm}-$ vs (CGC)U \langle , there is virtually no loss in activity from $\text{Cp}'_2\text{Ln}-$ to (CGC)U \langle catalysts. However, the ca. $10\times$ decrease in activity observed for **1** vs **2** reflects a Ln-like dependence on ionic radius in the sterically sensitive intramolecular 1,3-disubstituted allene HA/cyclization. Although substrates bearing geminal dialkyl substitutions were not investigated, the substantial increase in activity of both **1** and **2** for transformations **45**→**46** vs **47**→**48** (Table 7) is consistent with the more advantageous orientation of the reactive substrate moiety in the transition state owing to α -alkyl substitution.³⁸

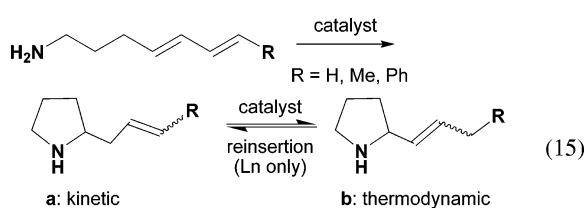
Although diastereoselectivity was not reported in detail for group 4 catalysts,^{5k,1} organolanthanides consistently afford 2,5-*trans*-pyrrolidine and 2,6-*cis*-piperidine heterocyclic products.³ⁱ In all instances, organoactinide catalysts (Table 7, entries 1–8) consistently favor 2,5-*trans*-pyrrolidine (**43**→**44**, precatalysts **1–6**) and 2,6-*trans*-piperidine (**45**→**46**, precatalysts **1** and **2**) diastereoselection. The former trend tracks that observed with organolanthanide catalysts and is explicable in terms of preferred orientation and minimization of unfavorable substrate–ancillary ligand steric repulsion. However, the latter result differs from that obtained with $\text{L}_2\text{Ln}-$ catalysts, likely reflecting the second, covalently bonded substrate interfering with C=C=C insertion at the An–N bond. Added steric obstruction in the already congested transition state (cf. **A** and **G**[‡]) is consistent with reduced diastereoselectivity and reduction in catalytic activity upon moving from coordinatively unsaturated (CGC)An \langle complexes, where diastereoselectivities up to 90% are achieved, to their less open **3–6** analogues, where diastereoselectivities are uniformly modest and reaction rates are markedly more sluggish.

(d) Aminodienes. While ample precedent exists for *intermolecular* 1,3-diene HA across the Periodic Table,^{2k} there have been few investigations of the intramolecular variant of this useful transformation. Notably, scope and mechanism have been thoroughly examined for Ln catalysts with diverse ancillary ligands, from conventional $\text{Cp}'_2\text{Ln}-$ to chiral bis(oxazolinato) complexes.^{3c,d,f} These studies reveal a dependence on Ln^{3+} ionic radius and coordinative unsaturation that is far more pronounced than in aminoalkene intramolecular HA/cyclization, where larger, more accessible metal centers with more open coordination spheres are optimal for rate and regioselectivity. Although recent computational studies⁴⁰ suggest that Ln–C σ -bond protonolysis following aminodiene cyclization may be turnover-limiting,⁴⁵ experimental data argue for turnover-limiting C–C unsaturation insertion into the Ln–N bond (Scheme 1),^{3c} as do

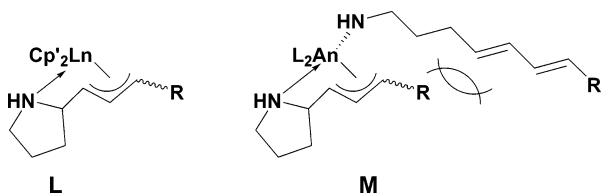
(45) Note that the marked dependence of the cyclization rate on ring size and significant C–C substituent electronic effects for alkene, alkyne, allene, and diene unsaturations seem to preclude turnover-limiting heterocycle protonolysis after C–C insertion into M–N (i.e., $k_{\text{protonolysis}} > k_{\text{insertion}}$ appears operative here).

computational results for aminoalkene and aminoalkyne HA/cyclization.³⁹

Intramolecular 1,3-aminodiene HA/cyclization, involving both terminal and 1,4-disubstituted (internal) diene units, is effectively catalyzed by (CGC)An complexes (Table 8). As for organo-4f-element catalysts, such transformations are efficient and highly regioselective. With the noteworthy exception of the 2-promoted **51**→**52a/b** conversion (vide supra), relative ring-closure rates follow expected trends where smaller pyrrolidines form more rapidly from unsubstituted 1,3-dienes than do piperidines, and 1,4-disubstituted diene conversions are slow vs those of terminal dienes.^{3c} This trend is typical of ring-closing reactions in general,^{38,41,46} and (CGC)An-catalyzed aminodiene HA is clearly governed by similar steric and electronic demands. Furthermore, product distributions typically favor thermodynamically less favored (~3 kcal/mol) terminal, monosubstituted olefinic products (**50a** and **52a**, Table 8). That product distributions are time-independent and favor the kinetic cyclization product (**a** in eq 15) suggests that subsequent isomerization via



reinsertion at the An center (**b** in eq 15) is unimportant, in contrast to most Ln-catalyzed transformations.^{3d} This trend for Ln catalysts is explicable in terms of well-precedented η^3 -allyl/benzyl intermediates (**L**)^{12,13} and suggests that such intermediates are more stable for large Ln³⁺ ions than for similarly sized An⁴⁺ ions, having two An–N σ -bonded substrates in the resting state (**M**).



The effects of ancillary ligand openness, as assayed by $\Delta\text{Cp}(c)\text{-M-L}$ (Chart 2) on the present An-catalyzed process (Figure 4d) parallel those in organolanthanide catalysis and those generally seen in Ln- or An-catalyzed aminoalkene HA/cyclization.^{2d,15} In contrast, the rate dependence on An⁴⁺ ionic radius (rate: U > Th) resembles more thermodynamically favored N–H bond additions to aminoalkyne C≡C and aminoallene C=C=C units. From a Hammond postulate standpoint,^{20,41} such behavior suggests a diene HA transition state more closely resembling reactants than products in each transformation class.

To rationalize organoactinide reactivity patterns for all HA reactions, it is beneficial to consider the estimated enthalpies associated with each class of cyclization (Table 9). For transformations where Scheme 2, step (i) is more exothermic vs step (ii), the U⁴⁺-catalyzed processes are more rapid; when steps (i) and (ii) are close in exothermicity (i.e., 1,2-disubstituted

alkenes), the rate dependence on metal ionic radius is negligible. In qualitative terms, the softer, more electron-rich substrates (i.e., alkynes > allenes > dienes) more rapidly undergo insertion at the slightly softer¹³ U⁴⁺ metal center, whereas the less soft alkene substrates more rapidly undergo insertion at the slightly harder¹³ Th⁴⁺ metal center. This ordering does not hold in organo-4f-element HA/cyclization,^{2d} suggesting that increased bond covalency^{12,13} may be operative in organoactinide vs organolanthanide catalysis.

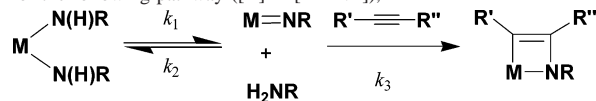
Mechanistic Implications. A priori, the present tetravalent organoactinide complexes could mediate catalytic intramolecular HA/cyclization via either of two distinct, limiting mechanistic scenarios: (1) a polar, highly organized four-centered, insertive transition state involving L₂An (species possessing two An–N σ -bonds (“Ln-like”; Scheme 2), or (2) a [2+2] cycloaddition pathway proceeding via reactive L₂An=NR species, analogous to that proposed for *intermolecular* alkyne HA with bulky amines, mediated by Cp₂MR₂, Cp₂M=NR(THF), and Cp′₂-AnMe₂ catalysts (M = Ti, Zr; An = Th, U) at elevated temperatures (Scheme 3).^{2a,e,f,h-n,47,48} In group 4 cases, scenario (2) has been shown to involve a rapid pre-equilibrium between Cp₂M[N(H)Ar]₂ and Cp₂M=NR(H₂NAr) (**B**) species, followed by turnover-limiting [2+2] RC≡CR′ cycloaddition to the Cp₂M=NR species (step (ii), Scheme 3), in agreement with the observed rate law (eq 16a).⁴⁷ Slightly different kinetics were reported for Cp′₂AnMe₂-catalyzed intermolecular additions of bulky and unhindered aliphatic 1° amines to terminal alkynes, although with zero-order dependence on [alkyne] (rates were independent of alkyne identity), suggesting rapid C≡C addition following turnover-limiting amine elimination, and with competing alkyne oligomerization processes.^{48,49} Although inconsistent with noncatalytic L₂An=NR chemistry,^{12–14,28,30} an alternative scenario can also be envisioned where an M=NR species forms irreversibly, followed by rapid C≡C addition (eq 16b).

In contrast, more active cationic U(NEt₂)₃⁺BPh₄[−] displays behavior similar to that of Cp′₂An[−] and Cp₂Zr[−]-catalyzed intermolecular terminal alkyne HA with 1° amines, but also mediates HNEt₂ addition to Me₃SiC≡CH,⁵⁰ precluding an obvious An=NR intermediate. Moreover, cationic organozir-

(47) (a) Baranger, A. M.; Walsh, P. J.; Bergman, R. G. *J. Am. Chem. Soc.* **1993**, *115*, 2753–2763. (b) Walsh, P. J.; Baranger, A. M.; Bergman, R. G. *J. Am. Chem. Soc.* **1992**, *114*, 1708–1719.

(48) (a) Straub, T.; Haskel, A.; Neyroud, T. G.; Kapon, M.; Botoshansky, M.; Eisen, M. S. *Organometallics* **2001**, *20*, 5017–5035. (b) Haskel, A.; Straub, T.; Eisen, M. S. *Organometallics* **1996**, *15*, 3773–3775.

(49) For the following pathway ([A] = [M=NR]),



$$\frac{d[A]}{dt} = k_1[M(\text{NHR})_2] - k_2[A][\text{RNH}_2] - k_3[A][\text{C}\equiv\text{C}] = 0$$

$$\Rightarrow k_2[A][\text{RNH}_2] + k_3[A][\text{C}\equiv\text{C}] = k_1[M(\text{NHR})_2]$$

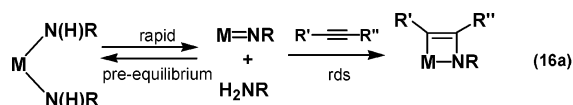
$$\therefore [A] = \frac{k_1[M(\text{NHR})_2]}{k_2[\text{RNH}_2] + k_3[\text{C}\equiv\text{C}]}$$

If the rate of product formation is $\nu = k_3[A][\text{C}\equiv\text{C}]$, then

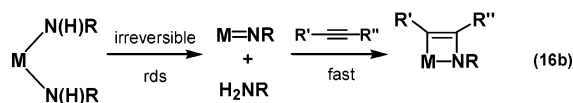
$$\nu = \frac{k_1 k_3 [M(\text{NHR})_2][\text{C}\equiv\text{C}]}{k_2[\text{RNH}_2] + k_3[\text{C}\equiv\text{C}]}$$

Therefore, (i) for k_3 very large, $\nu \sim [M(\text{NHR})_2]^1[\text{RNH}_2]^0[\text{C}\equiv\text{C}]^0$; (ii) for k_2 very large, $\nu \sim [M(\text{NHR})_2]^1[\text{RNH}_2]^{-1}[\text{C}\equiv\text{C}]^1$; and (iii) for k_3 very small, $\nu \sim [M(\text{NHR})_2]^1[\text{RNH}_2]^{-1}[\text{C}\equiv\text{C}]^1$.

(46) (a) Illuminati, G.; Mandolini, L. *Acc. Chem. Res.* **1981**, *14*, 95–102. (b) Mandolini, L. *J. Am. Chem. Soc.* **1978**, *100*, 550–554.



$$v \sim [\text{M}]^1 [\text{amine}]^{-1} [\text{alkyne}]^1$$



$$v \sim [\text{M}]^1 [\text{amine}]^0 [\text{alkyne}]^0$$

conium and organotitanium complexes effect *intramolecular* aminoalkene HA/cyclizations, with scope limited to 2° amine substrates, again suggesting that a *neutral* $\text{L}_2\text{M}=\text{NR}$ species cannot be an intermediate (eq 12).^{5h,i} Note that monomeric tetravalent actinide imido complexes are normally observed with sterically encumbered (e.g., $\text{Cp}'_2\text{An}(\text{O})$) ancillary ligands and result from bis(amido)actinide or related precursors (e.g., $\text{Cp}'_2\text{An}[\text{N}(\text{H})\text{Ar}]_2$ or $\text{Cp}'_2\text{An}(\text{Me})[\text{N}(\text{H})\text{Ar}]$) at elevated temperatures via α -H elimination.^{12–14,28,30,43,47,48} These considerations argue against the pathway of eq 16b, where the predicted rate law, although in agreement with the presently observed (intramolecular HA/cyclization) rate law, assumes a stable, monomeric $\text{L}_2\text{An}=\text{NR}$ intermediate. Under the mild reaction conditions typical of HA/cyclizations reported here, involvement of $\text{L}_2\text{An}=\text{NR}$ intermediates seems unlikely, considering the coordinative unsaturation of the (CGC)An \langle species involved, the reactivity of sterically unencumbered substrates, the facile 2° amine cyclizations, the absence of induction periods prior to catalytic turnover,³⁶ and the substantial rate differences observed for different C–C unsaturations. Furthermore, the rate *acceleration* at low [substrate] ($\text{L}_2\text{M}=\text{NR}$ formation favored) and rate *deceleration* at high [substrate] ($\text{L}_2\text{M}[\text{N}(\text{H})\text{R}]_2$ favored) seen in [2+2] cycloaddition pathways⁴⁷ are not observed here. On the contrary, (CGC)An \langle -mediated intramolecular 1° or 2° amine HA/cyclizations display opposing behavior (namely, high [product] moderately inhibits catalytic turnover via competitive binding; Figures 2 and 3)^{2d,3v,15} and exhibit the rate law $v \sim [\text{An}]^1 [\text{amine}]^0$ without an induction period, inconsistent with scenario (2) and signifying that turnover is not preceded by a rapid pre-equilibrium. Aminoalkene and aminoalkyne HA/cyclizations mediated by monosubstituted $\text{L}_2\text{M}(\text{NR}_2)\text{X}$ complexes, incapable of $\text{M}=\text{NR}$ formation with 1° or 2° amine substrates,¹⁶ further support mechanistic scenario (1), characterized by a highly organized transition state with turnover-limiting⁴⁵ C–C insertion into a σ -bonded $\text{M}-\text{N}$ species (cf. A). This is also in agreement with DFT-level computational studies of organolanthanide-mediated HA/cyclization.³⁹

Activation parameters derived for each C–C unsaturation (Table 9) also suggest a mechanistic pathway closely resembling that proposed for organolanthanide-mediated HA processes, where deviation from the generally preferred trivalent Ln^{3+} state is unlikely.¹³ Activation parameters for the present (CGC)An \langle -mediated HA/cyclizations are similar to those for the $\text{Cp}'_2\text{AnMe}_2$ -mediated *intermolecular* terminal alkyne HA ($\Delta H^\ddagger = 11.7(3)$ kcal/mol, $\Delta S^\ddagger = -44.5(8)$ eu).⁴⁸ The more negative ΔS^\ddagger is not unexpected in comparison to *intramolecular* aminoalkene ($\Delta H^\ddagger = 12.6(2)$ kcal/mol, $\Delta S^\ddagger = -29.6(3)$ eu) and aminoalkyne HA/cyclization ($\Delta H^\ddagger = 13.9(2)$ kcal/mol, $\Delta S^\ddagger = -27(5)$ eu; Table 9) processes and suggests that (CGC)An \langle -catalyzed intramolecular HA/cyclizations proceed through a transition state energetically similar to that postulated for Ln-catalyzed HA/cyclization (A). Activation parameters for (CGC)An \langle -catalyzed HA/cyclization are very similar to (within 3σ) those for Ln-catalyzed reactions (Table 9),^{2d,3} in accord with similar, highly organized insertive transition states. Additional mechanistic data and arguments will be published separately.¹⁶

Conclusions

The catalytic competence of readily accessible constrained geometry (CGC)An \langle (NR₂)₂ complexes in mediating intramolecular hydroamination/cyclization reactions of a large variety of primary and secondary amines tethered to multiple classes of terminal and disubstituted C–C unsaturations has been investigated in detail. The reaction scope includes aminoalkenes, aminoalkynes, aminoallenes, and aminodienes, with catalytic efficiencies comparable to those of the most active organolanthanide catalysts and *far exceeding* activities reported for most tetravalent transition metal complexes. Reactivity trends reveal a marked dependence on An^{4+} ionic radius and ancillary ligation, with pronounced reactivity enhancement afforded by the CGC framework, regardless of C–C unsaturation. Experimentally determined ΔH^\ddagger , ΔS^\ddagger , and E_a parameters are similar to those for organolanthanide-mediated processes, consistent with highly organized transition states exhibiting considerable bond-forming character. These facts, along with the rate law and other similarities to organolanthanide-catalyzed HA/cyclization processes, suggest a “Ln-like” σ -bond insertive mechanistic pathway proceeding through an An–N(H)R intermediate (Scheme 2).

Acknowledgment. We gratefully acknowledge the National Science Foundation (CHE-0415407) for funding this research. We also thank Ms. Charlotte L. Stern for collection and refinement of single-crystal X-ray diffraction data (ref 15).

Supporting Information Available: Full experimental details for substrate preparation, including improved synthetic procedures for **21**, **25**, and **41**, and (CGC)An \langle complexes. This material is available free of charge via the Internet at <http://pubs.acs.org>.

(50) Wang, J.; Dash, A. K.; Kapon, M.; Berthet, J.-C.; Ephritikhine, M.; Eisen, M. S. *Chem. Eur. J.* **2002**, *8*, 5384–5396.